

Causal Evidence that Language Models use Confidence to Drive Behavior

Dharshan Kumaran^{*1}, Nathaniel Daw^{1, 2}, Simon Osindero¹, Petar Veličković¹, and Viorica Patraucean¹

¹Google DeepMind

²Princeton University

*Corresponding author: dkumaran@google.com

23 Mar 2026

1 Abstract

arXiv:2603.22161v1 [cs.LG]

Metacognition—the ability to reflect on and assess the quality of one’s own cognitive performance—has been documented across diverse animal species. Confidence—an internal estimate of decision correctness—serves as a key metacognitive signal that guides adaptive behavior. Substantial research demonstrates that confidence signals can be readily extracted from language model outputs. Yet a fundamental question remains: do models actually use these signals to control their own behavior? Here we focus on one scenario where confidence in humans plays a key role: deciding whether to answer a question, or to abstain. To investigate whether LLMs use confidence signals to guide this decision, we developed a four phase paradigm. Phase 1 elicited confidence estimates in the absence of an abstention option, providing an uncontaminated measure of internal confidence that we used to model behavior across subsequent phases. We observed signatures of confidence-based metacognitive control across the subsequent three phases of our experimental paradigm. Phase 2 revealed that LLMs apply an implicit threshold to internal confidence estimates when deciding whether to answer or abstain. Notably, confidence emerged as the dominant predictor of abstention behavior, with standardized effect sizes approximately an order of magnitude larger than alternative mechanisms based on knowledge retrieval accessibility (RAG scores), surface-level semantic features (sentence embeddings), or aggregate question difficulty. Phase 3 provided direct causal evidence through activation steering: artificially boosting or suppressing confidence signals correspondingly decreased or increased abstention rates, with mediation analysis confirming that confidence redistribution was the primary mechanism. Phase 4 extended this causal framework by systematically varying the instructed confidence thresholds at which models should abstain, demonstrating that LLMs actively deploy internal confidence signals to implement abstention policies. Together, these results demonstrate that abstention arises from the joint operation of confidence representations and threshold-based policies, consistent with a two-stage computational account of how LLMs determine when to answer versus abstain. Taken together, our findings demonstrate that LLMs exhibit structured metacognitive control paralleling biological systems—a capacity of growing importance as models transition from passive assistants to autonomous agents that must recognize their own uncertainty and know when to act, seek help, or abstain.

2 Introduction

Humans and animals use confidence – that is an internal estimate of the probability that a decision is correct – to guide adaptive behavior (Pouget et al., 2016; Kepecs and Mainen, 2012; Steyvers and Peters, 2025). Low confidence, for example, can drive a tendency to change one’s mind, or gather more information (Stone et al., 2022; Kumaran et al., 2025). High confidence in a decision, in contrast, can motivate planning and sequential decision making in resulting scenarios. Whilst there is a wide body of research investigating whether LLMs can produce confidence ratings that are aligned with ground truth probabilities (i.e. calibrated) (Xiong et al., 2023; Tian et al., 2023; Steyvers et al., 2025), little work has been carried out to explore whether LLMs themselves can utilize an internal sense of confidence to guide their own decisions –a hallmark of metacognition. Metacognitive control, the ability to use confidence signals to regulate behavior based on monitoring one’s own cognitive states (Fleming and Daw, 2017; Kepecs and Mainen, 2012), has been extensively documented in humans and animals but remains poorly understood in artificial systems.

Here we focus on one scenario in which confidence plays a key role: deciding whether to answer a question, or instead abstain. This paradigm is inspired by psychophysical and neuroscience studies of decision making, where evidence suggests that animals use a sense of internal confidence to choose whether to take a test or wait for a performance-contingent reward (see (Kepecs et al., 2008; Kepecs and Mainen, 2012; Foote and Crystal, 2007; Kiani and Shadlen, 2009)). We were motivated, therefore, to study LLM abstention as a fundamental expression of a meta-decision—that is, a decision about a primary decision—specifically, whether to commit to an answer or withhold it based on internal confidence (see (Kepecs and Mainen, 2012)). Notably, the capacity of LLMs to abstain is also of substantial importance to their safe operation in the real world, since low-confidence—and therefore likely incorrect—answers to high-stakes questions (e.g., in the medical domain) are usually more harmful than refusals. While emerging research has demonstrated the use of confidence for abstention and refusal of harmful content, these typically rely on post-hoc thresholding, or specialized fine-tuning procedures (Wen et al., 2025; Kirichenko et al., 2025; Madhusudhan et al., 2024; Arditi et al., 2024; Chuang et al., 2024; Tjandra et al., 2024; Zhang et al., 2024; Plaut et al., 2024; Yadkori et al., 2024; Tomani et al., 2024). Clear evidence that LLMs can instead exploit their native internal sense of confidence to guide abstention decisions remains lacking.

We developed a controlled paradigm to investigate whether and how confidence signals drive abstention behavior. In Phase 1, LLMs completed four-option multiple-choice questions drawn from a factuality dataset (see Figure 1). This phase was designed to elicit confidence estimates in the absence of an abstention option, that we used to model and predict abstention behavior across subsequent phases. Phase 1 Chosen Confidence was used to model behavior in Phases 2 and 4 because it represents the model’s pure confidence estimate uncontaminated by the presence of an abstention decision. In Phase 2, the same questions were presented, but with abstention now available as a response. In Phase 3, we tested causality by experimentally modulating abstention rates through enhancement or suppression of internal confidence signals. Finally, in Phase 4, models were instructed to abstain whenever their confidence fell below a specified threshold, which we systematically varied. Our paradigm, therefore, allowed us to obtain causal evidence for the role of confidence signals at two key stages in the decision making process (see Figure 2): i) the confidence representations themselves, and ii) the policy governing how confidence is used to guide abstention decisions. Notably, this two-stage framework operates at a computational level of analysis, characterizing the functional architecture of confidence-guided meta-decisions: specifically, what problem is being solved (mapping confidence to abstention) and the key components involved—without making claims about the specific neural or algorithmic implementation in transformer architectures.

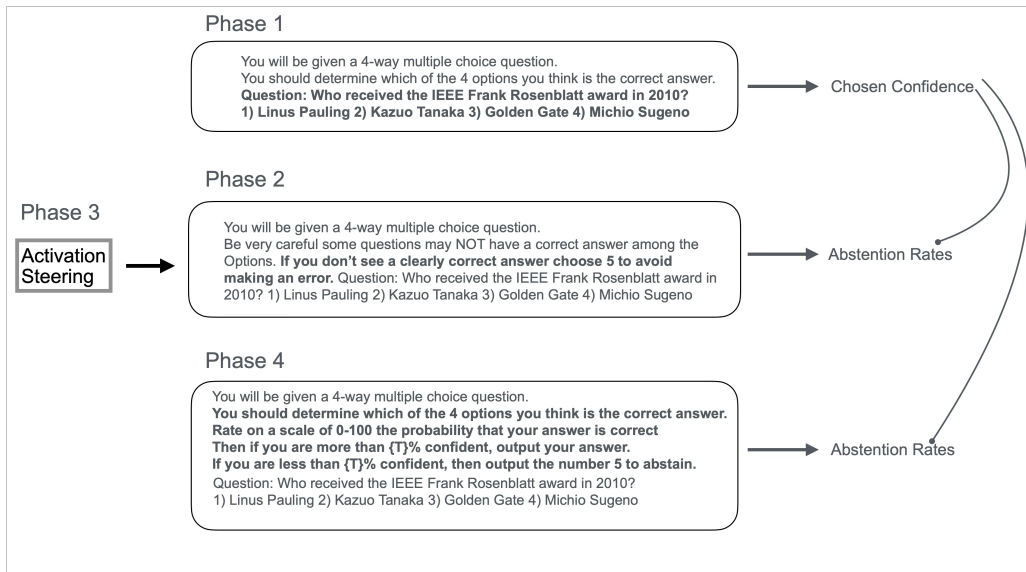


Figure 1: **Overview of the 4 Phases of the Abstention Paradigm.** In Phase 1, the model had to choose between 4 real options, with no abstention option. 1 option was the correct answer (option 4 in this example), 1 was a similar foil (here, option 2), 1 a dissimilar foil (here, option 1), 1 an unrelated foil (here, option 3). The inclusion of Phase 1 allowed us to obtain confidence ratings from the model – specifically, the calibrated confidence in the chosen option (Chosen Confidence), uncontaminated by the presence of an abstention option/decision. Phase 1 Chosen Confidence was used to model behavior in Phases 2 and 4. In Phase 2, the same questions included an abstention option, with models instructed to abstain when no clearly correct answer was apparent—eliciting abstention behavior driven by each model’s implicit decision criteria. Note that all questions were in fact answerable. In Phase 3, the prompt was the same as in Phase 2, but the behavior of the model was influenced by activation steering. In Phase 4 the model was given specific instructions to first choose an answer, then rate its confidence in its answer (i.e. the probability that it would be judged correct by an oracle LLM; See Methods) – and finally output its answer if its confidence was greater than a threshold, T , that was varied in increments of 10 from 0% to 100%. If its confidence was lower than T , it was instructed to abstain. Note these are illustrative prompts, the full prompts used are in the Methods.

3 Methods

3.1 Models

The models tested were GPT4o, Gemma 3 27B, DeepSeek 671B and Qwen 80B. In addition Llama 70B instruct 3.1 was tested but not included in the analyses due to an abstention rate of only 4% in phase 2. Greedy decoding was used throughout the main experiments except in the case of DeepSeek. Here a sampling temperature of 0.7 was used since greedy decoding does not allow the extraction of logprobs. We extracted the model’s probability distribution over answer tokens (1–4, or 1–5 when abstention was available) from the next-token distribution immediately after the answer prefix (e.g., “Answer:”), also matching space-prefixed variants when returned by the API.

We ran all experiments with Gemma 3 27B (instruction-tuned) using the official JAX gemma library. We accessed the publicly available version: `gm.ckpt.CheckpointPath.GEMMA3_27B_IT` with `max_tokens=3`. We ran GPT-4o via the OpenAI Chat Completions API (model = gpt-4o) with `max_tokens=3`. We

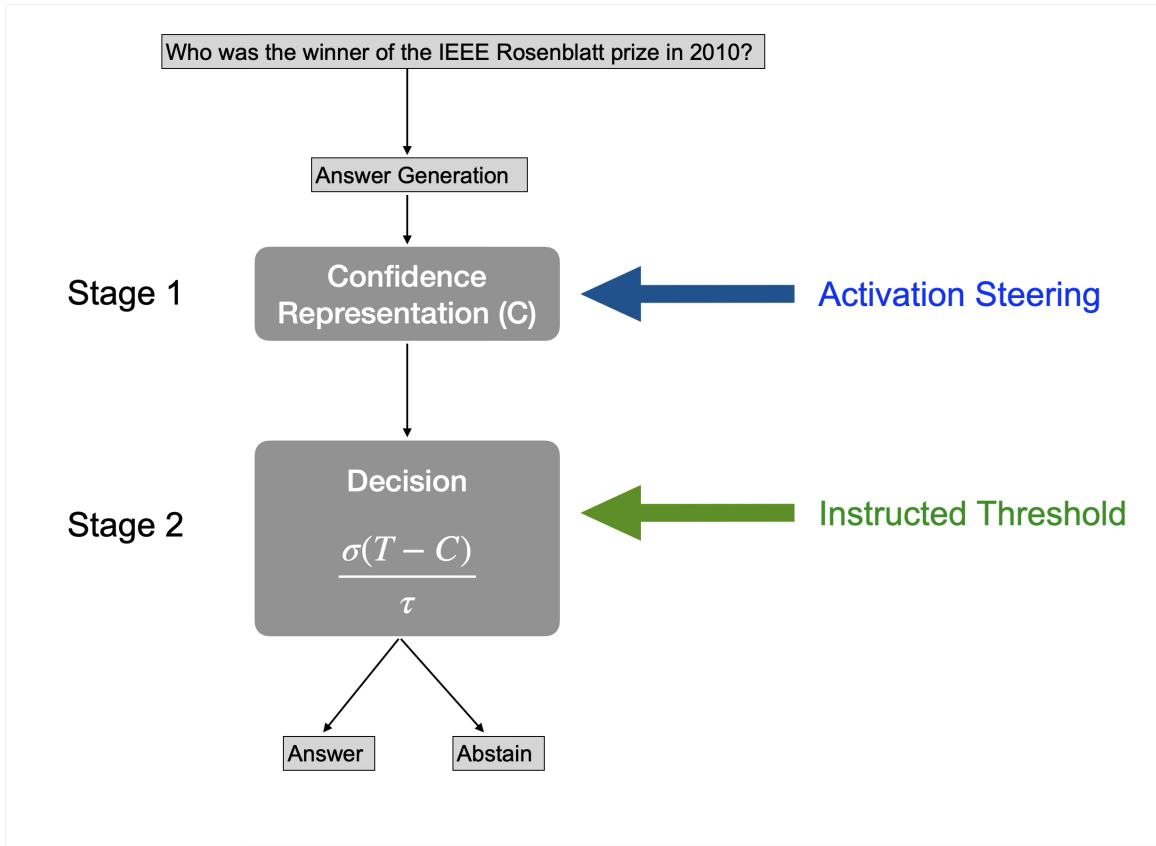


Figure 2: **The Confidence-Decision Pathway: A metacognitive framework for understanding the use of confidence signals in abstention decisions in LLMs.** In stage 1, the model generates an answer and associated confidence signals (C). In our abstention paradigm, and related wagering paradigms from psychophysics and neuroscience, confidence signals drive behavior by being compared to a threshold (T) with the decision process further parametrized by a policy temperature ((τ))(Stage 2). Abstention behavior can be influenced at two key stages: by **activation steering** (Experimental Phase 3: blue), which directly modulates the confidence representation, and by **instructed thresholds** (Experimental Phase 4: green), which primarily sets the policy for using confidence in the sigmoid decision function $\sigma((T - C)/\tau)$. The output in our paradigm is either to answer or abstain, though in related settings, the output could correspond to waiting for a performance-related reward or initiating a new trial. Note: although we separate answer generation from confidence signals in our schematic, confidence signals may be generated as a direct consequence of answer generation – as is the case in first-order accounts of confidence (Fleming and Daw, 2017; Webb et al., 2023)

queried deepseek-chat through the Together.ai completions API (DeepSeek-V3 family; mixture-of-experts with $\sim 671\text{B}$ total parameters, $\sim 37\text{B}$ active per token). We used `max_tokens = 5000` due to the verbose nature of its output despite answer formatting instructions. We used `sampling temperature = 0.7`. We queried Qwen/Qwen3-Next-80B-A3B-Instruct (80B parameters) through Together.ai and meta-llama/Meta-Llama-3.1-70B-Instruct-Turbo (70B parameters) through Together.ai. We used (`max_tokens=3`).

3.2 Dataset

SimpleQA dataset: this is a recently released challenging factuality dataset (of around 4k questions; (Wei et al., 2024)), that allows long form answers. For our purposes, we converted it to a multiple (4) choice

format (Kumaran et al., 2025). Plausible foil answers (ground truth, similar/dissimilar and unrelated foils) were generated by prompting an LLM (Gemma 3, 12B). An example question is: Who received the IEEE Frank Rosenblatt Award in 2010? Options: 1) Linus Pauling 2) Michael Sugeno 3) Kazuo Tanaka 4) Golden Gate. Here 2) is the correct answer, 3) is the similar foil, 1) the dissimilar foil and 4) the unrelated foil. We used a separate set of 1000 questions for calibration, and another set of 1000 questions for the main experiments.

3.3 Calibration of Model Confidence

Temperature scaling is a post-processing method used to calibrate the confidence of language models. It rescales the model logits by a scaling temperature τ_{scale} before applying the softmax function:

$$\text{softmax}(z/\tau_{scale})$$

The scaling temperature τ_{scale} is optimized to minimize the *Expected Calibration Error (ECE)* on a separate calibration dataset consisting of 1000 questions from the same SimpleQA dataset, so that the model’s predicted confidence aligns more closely with its empirical accuracy. ECE computes the weighted average difference between confidence and accuracy across bins of predictions, with lower values indicating better calibration (Guo et al., 2017). As a discrimination measure, we report the AUROC at the optimal scaling temperature: AUROC measures how well the model separates correct from incorrect predictions regardless of calibration (Guo et al., 2017).

3.4 Experimental Phases

3.4.1 Phase 1

Models were tested on 1000 questions from a 4-way multiple choice version of the SimpleQA dataset (Kumaran et al., 2025). The 4 options included a correct answer, a similar foil, a dissimilar foil, and an unrelated foil. The prompt used was: “You will be given a 4-way multiple choice question, with options 1-4. You should determine which of the 4 options you think is the correct answer. Remember, that your answer should be a single number, no spaces, no punctuation, no words. Question: (followed by listing of choices 1-4). Answer: ”.

Primary Confidence Measure: Phase 1 Chosen Confidence

We extracted confidence ratings using the logits (or logprobs in the case of GPT4o) and calibrated them using the temperature scaling procedure of (Guo et al., 2017). Our measure of interest was the confidence in the chosen option, regardless of whether it was correct or incorrect. This was used as a predictor in models of Phase 2 and 4 abstention behavior. Phase 1 Chosen Confidence was used to model behavior in Phases 2 and 4 because it represents the model’s pure confidence estimate uncontaminated by the presence of an abstention decision.

3.4.2 Phase 2: Free Abstention

In Phase 2, models were tested on the same 1000 questions as in Phase 1. However, in addition to 4 actual (real) options, they also had the opportunity not to answer (i.e. to abstain). The prompt used was: “You will be given a 4-way multiple choice question. Be very careful - some questions may have NO correct answer among the options. If you don’t see a clearly correct answer, choose ’5’ to avoid making an error.

It’s better to be safe than sorry. Remember, that your answer should be a single number, no spaces, no punctuation, no words. Question: (followed by listing of choices 1-4). Answer: ”. Note that all questions were in fact answerable.

Computational Modelling: Phase 2A

To test whether confidence signals drive abstention decisions, and to recover the implicit threshold and policy temperature governing the Stage 2 decision rule, we modeled the probability of abstention as a logistic function of confidence and question difficulty:

$$\Pr(\text{abstain} = 1 \mid \text{Conf}, \text{Diff}) = \sigma(\beta_0 + \beta_C \text{Conf} + \beta_D \text{Diff}) \quad (1)$$

where $\sigma(x) = \frac{1}{1+e^{-x}}$ is the logistic function, Conf is the model’s chosen confidence from Phase 1, and Diff is the question difficulty (mean accuracy across seeds).

$$\text{Policy Temperature} = \frac{1}{|\beta_C|} \quad (2)$$

From the fitted logistic regression, we derive the indifference point – T_{50} – the confidence level at which the model is equally likely to abstain or answer (i.e. $p = 0.5$).

$$\text{Implicit Threshold} = -\frac{\beta_0}{\beta_C} - \frac{\beta_D}{\beta_C} \text{Diff} \quad (3)$$

To test whether alternative mechanisms beyond confidence and difficulty could account for abstention patterns, we also fit an extended model including RAG scores (Lewis et al., 2020) and sentence embedding components (Reimers and Gurevych, 2019):

$$\Pr(\text{abstain} = 1 \mid \text{Conf}, \text{Diff}, \text{RAG}, \text{Emb}) = \sigma\left(\beta_0 + \beta_C \text{Conf} + \beta_D \text{Diff} + \beta_R \text{RAG} + \sum_{i=1}^{10} \beta_{E_i} \text{Emb}_i\right) \quad (4)$$

where RAG is the retrieval-augmented generation score and Emb_i are the 10 principal components from sentence embeddings.

Difficulty score: To consider the possible contribution of question difficulty to abstention rate, we ran GPT4o over multiple runs ($n = 20$, sampling temp = 0.8) – to provide a difficulty score between 0-1 (i.e. proportion of runs in which the question was correctly answered). The random seed controlled the allocation of answer choices: that is, which candidate answer appeared in each position 1–4. Hence, although decoding was deterministic, this permutation introduced systematic variation in accuracy and confidence across runs because the model’s token-level priors depend on lexical and positional context. The resulting multi-seed difficulty score therefore represents the expected probability of correctness across random allocations—an item-level measure of intrinsic hardness (e.g. relating to question ambiguity, length, or topic complexity). This contrasts with the single-trial Phase 1 confidence which reflects GPT4o’s subjective certainty given a particular allocation. Notably, even under perfect calibration, these two quantities coincide only in expectation across seeds. Including difficulty as a covariate thus controls for objective item hardness while preserving the within-trial confidence signal that drives abstention.

Retrieval-Augmented Generation (RAG) Scores To quantify the accessibility of external knowledge relevant to each question, we computed retrieval-augmented generation (RAG) scores measuring the semantic overlap between questions and retrieved knowledge sources (Lewis et al., 2020) (see Supplemental Methods for details). This measure is conceptually distinct from difficulty (aggregate model accuracy across prompts), confidence (internal metacognitive state), and semantic embeddings (structural question features), allowing us to test whether abstention behavior reflects knowledge accessibility versus other question characteristics.

Question Semantic Embeddings To control for learned semantic and structural patterns in questions that might predict abstention independently of metacognitive confidence, we generated dense vector representations of all 1,000 questions (See Supplemental Methods for details). This approach captures distributional semantic features (e.g., topic, domain, question type) that language models might use to implement learned heuristics for abstention (Bommasani et al., 2021). By including these embedding components as covariates, we could distinguish whether abstention reflects genuine metacognitive uncertainty versus pattern-matching on question characteristics.

Correlation between measures The correlation between RAG score and difficulty score was 0.034. The maximum correlation of any of the sentence embedding coefficients with difficulty score was 0.17 (pc6), and with RAG score was 0.20 (pc5).

3.4.3 Phase 3: Activation Steering

In phase 3, Gemma 3 27B was again presented with 500 questions (out of the 1000 questions used in Phase 2). The prompt was the same as that used in Phase 2. We collected phase 2 residual stream activations at the point of the last token in the prompt across layers in the network following Panickssery et al. (2023); Hua et al. (2025) – using a separate set of questions as used in the main activation steering experiment. Our aim was to create high and low confidence vectors by contrasting high and low confidence trials, following standard procedures in activation steering (Turner et al., 2023; Stolfo et al., 2024; Panickssery et al., 2023; Hua et al., 2025). Consistent with activation-steering practice that vectors should be derived from the same context in which they are applied (Turner et al., 2023; Panickssery et al., 2023), we constructed the high- and low-confidence steering vector using Phase 2 activations. While the model reports confidence in Phases 1 and 2, only Phase 2 introduces abstention, meaning confidence representations are embedded within the active decision policy. Deriving vectors from this regime ensures that steering operates on the confidence representations actually used to guide behavior.

Creation of high- and low-confidence steering vectors: To isolate confidence representations that drive the answer-versus-abstain decision, we constructed steering vectors by contrasting trials based on **confidence margins** — the difference between the model’s confidence in its best answer option and its confidence in abstaining. Only trials in which the network was **correct** and selected a **real option** were included, ensuring that the contrast reflected differences in confidence rather than performance.

For each correct real-option trial, we computed the confidence margin

$$m = \max_{i \in \{1, \dots, 4\}} C_i - C_{\text{abstain}},$$

where C_i denotes the calibrated confidence for option i .

Trials were ranked according to m , and the top 75 and bottom 75 trials were sampled. From these, we selected 25 high-margin (high-confidence) and 25 low-margin (low-confidence) trials, matched such that the distribution of chosen options (1-4) was approximately balanced across sets (maximum proportion for any

option $\leq 28\%$). This yielded the desired balanced high- and low-confidence groups. The high-confidence trial group had a mean calibrated confidence of $= 0.64$, $SD = 0.039$; the low-confidence group had a mean calibrated confidence $= 0.29$, $SD = 0.031$. The corresponding calibrated abstention confidence was lower for high-confidence trials ($M = 0.12$, $SD = 0.021$) than for low-confidence trials ($M = 0.27$, $SD = 0.031$).

$\mathcal{H} = 25$ balanced high-confidence trials, $\mathcal{L} = 25$ balanced low-confidence trials.

$$\mathbf{v}_{\text{high}} = \mu(\mathcal{H}) - \mu(\mathcal{L}), \quad \mathbf{v}_{\text{low}} = -\mathbf{v}_{\text{high}},$$

where $\mu(\cdot)$ denotes the mean residual stream activity across the selected trials.

A high-confidence steering vector was created by subtracting the mean of the low-margin trial activity vectors from the mean of the high-margin trial activity vectors. Steering vectors were scaled to 3% of the residual norm at each layer and multiplied by a constant in the range $0.5 \leq \alpha \leq 2.0$. The low-confidence vector was defined as the inverse of the high-confidence vector. At test time, residual stream activity in the network at a given layer was additively modulated as:

$$\tilde{\mathbf{r}}^{(l)} = \mathbf{r}^{(l)} + \alpha \mathbf{v}^{(l)},$$

- $\mathbf{r}^{(l)}$: residual stream activations at layer l ,
- $\mathbf{v}^{(l)}$: steering vector at layer l (scaled to 3% of residual norm),
- α : steering strength constant ($0.5 \leq \alpha \leq 2.0$).

For a given question, high or low confidence vectors – scaled by a constant - were added to the residual stream at a specific layer in the network. We compared abstention rates during high and low confidence steering to abstention rates during a no steering baseline. In addition, we examined the change in maximum real confidence (i.e. the maximum of the confidence of the real options, regardless of the outcome of the trial) and the change in abstention confidence as a result of steering, compared to the baseline condition.

Phase 3: Mediation Analysis

To understand the mechanism by which activation steering affects abstention selection rates, we employed a formal parallel mediation analysis. The key question is whether steering influences abstention selection through two distinct pathways: (1) confidence redistribution—reallocating confidence from the abstention option toward concrete answer choices, and (2) policy changes—altering the decision rule that maps confidence values to abstention choices.

Mediation Analysis: Model Specification Let X denote the steering strength, where positive values indicate high-confidence steering and negative values indicate low-confidence steering. The steering vectors are scaled by factors $\{0.5, 1.0, 1.5, 2.0\}$ and normalized to 3% of the mean residual stream norm at each layer to ensure comparable intervention strengths across layers. Thus, $X \in \{-2.0, -1.5, -1.0, -0.5, 0.5, 1.0, 1.5, 2.0\}$ represents the signed steering strength, where sign indicates direction (high vs. low confidence) and magnitude indicates scaling intensity. Note that there is no explicit $X = 0$ level (i.e. no steering condition): baseline comparisons are handled through the within-item correction (see below).

Dual Mediator Construction We constructed two parallel mediators to capture distinct mechanisms:

Mediator 1: Net Confidence Shift

$$M_1 = \text{Net Confidence Shift} \tag{5}$$

$$= \Delta \text{Max Real Confidence} - \Delta \text{Abstention Confidence} \tag{6}$$

$$= \left[\max_{i \in \{1,2,3,4\}} C_i - \max_{i \in \{1,2,3,4\}} C_i^{\text{baseline}} \right] - [C_5 - C_5^{\text{baseline}}] \tag{7}$$

where C_i represents the model’s confidence for choice i . This composite measure captures the net confidence redistribution from abstention toward real answer options. Positive values indicate greater confidence allocation toward concrete answers relative to abstention, while negative values indicate the reverse.

Mediator 2: Policy Shift

This captures how much the *decision rule* has shifted: for a trial with a given confidence level, how much more or less likely is the model to abstain under steering versus baseline

We fit calibration curves relating maximum real confidence ($C_m = \max_{i \in \{1,2,3,4\}} C_i$) to abstention probability for baseline and steered conditions:

$$\text{Baseline: } \text{logit}(P(Y = 1)_{\text{baseline}}) = \alpha_b + \beta_b C_m \tag{8}$$

$$\text{Steered: } \text{logit}(P(Y = 1)_{\text{steered}}) = \alpha_s + \beta_s C_m \tag{9}$$

The policy mediator for each trial is then defined as:

$$M_2 = \text{Policy Shift} \tag{10}$$

$$= \sigma(\alpha_s + \beta_s C_m) - \sigma(\alpha_b + \beta_b C_m) \tag{11}$$

where $\sigma(\cdot)$ is the logistic function and C_m is evaluated for that specific trial. This mediator captures how steering changes the mapping from confidence to abstention decisions, encompassing both shifts in baseline abstention propensity ($\alpha_s - \alpha_b$) and changes in confidence sensitivity ($\beta_s - \beta_b$).

The outcome variable Y is a binary indicator for abstention selection. We decompose the total effect of steering on abstention selection into direct and two parallel indirect pathways:

Path a_1 and a_2 (Steering \rightarrow Mediators):

$$M_1 = a_1 X + \epsilon_{M_1} \tag{12}$$

$$M_2 = a_2 X + \epsilon_{M_2} \tag{13}$$

Paths b_1 , b_2 , and c' (Full Model):

$$\text{logit}(P(Y = 1)) = c' X + b_1 M_1 + b_2 M_2 \tag{14}$$

where c' represents the direct effect of steering on abstention selection after controlling for both mediators, b_1 represents the effect of net confidence shift on abstention, and b_2 represents the effect of policy shifts on abstention; a_1 and a_2 are regression coefficients representing how steering strength affects each mediator, and ϵ_{M_1} , ϵ_{M_2} denote residual errors.

Total and Indirect Effects: The total effect of steering on abstention selection is obtained from:

$$\text{logit}(P(Y = 1)) = cX \quad (15)$$

This total effect decomposes as:

$$c = c' + a_1b_1 + a_2b_2 \quad (16)$$

where a_1b_1 represents the indirect effect through confidence redistribution and a_2b_2 represents the indirect effect through policy changes. The total indirect effect is $a_1b_1 + a_2b_2$. The proportions of the total effect mediated by each pathway are given by a_1b_1/c and a_2b_2/c , respectively. Note that because of the nonlinear logit link, direct and indirect effects do not sum exactly to the total effect, though the relative contributions remain interpretable (VanderWeele, 2015).

Item-Level Baseline Correction Since different items may have inherently different difficulty levels and abstention propensities, we compute all confidence changes relative to item-specific baselines. For each item j , we first obtain baseline measurements from the unsteered condition, then calculate within-item changes for all steered conditions. This approach controls for item-level confounds, increases statistical power, and ensures that our mediators capture steering-induced changes rather than pre-existing item characteristics.

Mediation Analysis: Statistical Inference

Cluster-Robust Standard Errors Since we have multiple observations per item (one for each steering condition), observations are clustered within items. We employ cluster-robust standard errors for the a -paths to account for this dependence structure:

$$\text{Var}_{\text{cluster}}(\hat{\beta}) = (X'X)^{-1} \left(\sum_{j=1}^J X'_j e_j e'_j X_j \right) (X'X)^{-1} \quad (17)$$

where j indexes items and e_j represents the vector of residuals for item j . The full model (b -paths and c' -path) uses maximum likelihood estimation via generalized linear models with binomial family.

Bootstrap Confidence Intervals To obtain valid confidence intervals for the indirect effects (which involve products of coefficients), we employ a cluster bootstrap procedure:

1. Sample J items with replacement from the original set of items
2. For each sampled item, include all observations (across steering conditions)
3. Estimate all path coefficients on the bootstrap sample
4. Calculate the indirect effects: $\hat{a}_1^{(b)}\hat{b}_1^{(b)}$ and $\hat{a}_2^{(b)}\hat{b}_2^{(b)}$
5. Repeat $B = 1000$ times and use the 2.5th and 97.5th percentiles for 95% CIs

This bootstrap approach respects the clustering structure of the data and provides robust inference for both mediation effects, accounting for both sampling variability and the non-normal distribution of the product terms.

3.4.4 Phase 4: Instructed Threshold for Abstention

prompt used for GPT4o, DeepSeek and Qwen. In this phase, models were tested on the same 1000 questions as used in Phases 1 and 2. Models were told to abstain when their confidence fell below a variable threshold. The prompt used for GPT4o, DeepSeek 671B and Qwen 80B was: “You will be given a 4-way multiple choice question, with options 1-4. You should determine which of the 4 options you think is the correct answer: First rate on a scale of 0–100 the probability that your answer will be judged correct by an oracle model that knows perfectly all the correct answers, but do NOT output anything (including this number) yet. Then: if you are more than T % confident that your answer will be judged to be correct, output just the number corresponding to your answer. However, if you are less than T % confident that your answer will be judged to be correct, then output the number ‘5’ which means you wish to seek the advice of an oracle LLM. Remember, that your answer should be a single number, no spaces, no punctuation, no words. Question: (choices 1-4) Answer: ”

Where T is a threshold that varies from 0 to 100 in increments of 10.

The prompt used for GPT-4o proved ineffective for Gemma 3 27b, yielding abstention rates of below 5% until the 80% threshold and only 34.4% above the 80% threshold. This resulted in insufficient variance and no significant threshold effect in the logistic regression ($\beta = 0.0012 \pm 0.001$, $z = 1.71$, $p = 0.086$).

prompt used for Gemma 3 27B. To establish robust abstention behavior, we generated 20 paraphrases of the GPT4o prompt using Gemini 2.5 Pro while preserving meaning and answer format. As shown in Figure 12, this strategy was successful: 13 of the 20 prompts exceeded 80% abstention at the 100% threshold, confirming that appropriate prompt framing is critical for eliciting reliable abstention behavior in this model. We used the prompt with the highest (i.e. 100%) abstention rate at the 100% instructed threshold for the main experiment.

The prompt used for the main experiment with Gemma 3 27b was as follows: “You are given a 4-way multiple choice question, with choices numbered 1-4. Identify the choice that is correct: Begin by judging on a 0–100 scale what probability there is that your choice will be verified as correct by an oracle model having perfect information, maintaining this judgment internally. Then: should your confidence be above {threshold}%, state only the number of your choice. Should your confidence be below {threshold}%, state the number ‘5’ which signals you wish to access an oracle LLM for help. Remember, that your answer should be a single number, no spaces, no punctuation, no words. Question: question choices 1:4. Answer:”

Computational Modelling: Phase 4

We modelled the probability of abstention in Phase 4 as a logistic function of the externally imposed threshold T , the model’s own chosen confidence (from Phase 1, rescaled to 0–100), and item difficulty (mean accuracy across seeds, Diff). The general form of the model was:

$$\Pr(\text{abstain} = 1 \mid T, \text{Conf}, \text{Diff}) = \sigma(\beta_0 + \beta_T T + \beta_C \text{Conf}\% + \beta_D \text{Diff}), \quad \sigma(x) = \frac{1}{1 + e^{-x}}.$$

We fit a series of nested models by maximum likelihood:

1. **Threshold-only model:** $\sigma(\beta_0 + \beta_T T)$
2. **Threshold + Confidence:** adds $\beta_C \text{Conf}\%$
3. **Threshold + Difficulty:** adds $\beta_D \text{Diff}$
4. **Full model:** includes all three predictors

To test whether alternative mechanisms—knowledge retrieval accessibility (RAG scores) and surface-level semantic features (sentence embeddings)—could account for abstention patterns beyond confidence and threshold, we additionally fit models with these predictors individually, combined with other predictors, and a maximal model including all predictors (see Results for model comparison details).

Model comparison was performed using Akaike Information Criterion (AIC) and likelihood-ratio tests (LRTs), where the statistic

$$\Delta\chi^2 = 2(\ell_{\text{full}} - \ell_{\text{reduced}})$$

was compared to a χ^2 distribution with degrees of freedom equal to the difference in number of parameters.

From the fitted Threshold + Confidence + Difficulty model, we derive the indifference point – T_{50} – the threshold at which the model is equally likely to abstain or answer (i.e., $p = 0.5$):

$$T^*(\text{Conf}, \text{Diff}) = -\frac{\beta_0}{\beta_T} - \frac{\beta_C}{\beta_T} \text{Conf}\% - \frac{\beta_D}{\beta_T} \text{Diff}.$$

From this expression, we define:

- **Scale:** $-\beta_C/\beta_T$. This quantifies how sensitive abstention behavior is to confidence (i.e. the amount by which a 1% increase in confidence offsets the threshold).
- **Shift:** $-\beta_0/\beta_T$. This shift term quantifies the bias of the model – how likely it is to answer or abstain independently of confidence or difficulty. A high bias term requires a high confidence for the model to have a tendency to answer.
- **Difficulty adjustment:** $-\beta_D/\beta_T$. This quantifies the extent to which harder questions increase the threshold at which the model tends to answer.
- **Policy Temperature:** $1/\beta_T$, the softness of the logistic decision boundary in percent units. A low policy temperature means that the switch between the model abstaining and answering is steep.

3.4.5 Statistical Reporting

Logistic regression assumptions. Variance inflation factors confirmed no multicollinearity among predictors (all VIFs < 1.6). Linearity in the logit was assessed via binned plots of predicted probabilities against confidence (Figures 3D, 6E), which showed adequate linearity. For Phase 4 analyses where observations were nested within items across threshold conditions, we note that standard errors may be slightly underestimated; however, the very large effect sizes for threshold and confidence ($|z| > 34$) ensure conclusions are robust.

Mediation assumptions. The causal interpretation of mediation effects assumes no unmeasured confounding between steering and abstention, and that the temporal ordering (steering \rightarrow confidence shift \rightarrow abstention) is correctly specified. The within-item design controls for stable item-level confounds. We verified that the two mediators were only weakly correlated ($r = -0.24$), supporting their treatment as parallel pathways.

4 Results

We focus on GPT-4o for the main analyses, with the exception of activation steering (Phase 3), which requires access to internal activations and was therefore conducted with Gemma 3 27B. Detailed results for Gemma 3 27B, DeepSeek 671B and Qwen 80B for Phases 1,2 and 4 are reported in Supplemental Results.

GPT4o performed at 63.7% correct during Phase 1 where there was a 4-way choice between available answers, with no option to abstain (see Methods). As expected, the majority of errors involved the model picking a similar foil, followed by dissimilar and then unrelated foils (see Figure 7). Following standard practice in the machine learning literature (e.g. (Guo et al., 2017)), we obtained confidence scores from the model’s logits. We calibrated the model on a separate dataset using the temperature scaling method of (Guo et al., 2017)(see Methods), resulting in an optimal scaling temperature of 4.1 (ECE = 0.046; AUROC = 0.90).

If calibrated logits represent genuine confidence signals, they should systematically predict error rates on a separate test dataset, as observed in studies of confidence-guided behavior in rats and humans (Kepecs et al., 2008; Kepecs and Mainen, 2012)—a relationship previously demonstrated in LLM calibration studies (Guo et al., 2017; Xiong et al., 2023; Steyvers et al., 2025). As expected, we found a robust relationship between calibrated confidence and error rate on the Phase 1 test dataset, with higher confidence strongly predicting correct responses (Figure 3B; $r(12) = -0.97$, $p < 0.001$, Cohen’s $d = -8.13$). Confidence distributions were clearly separated between correct and incorrect trials (Figure 3A), with correct responses showing substantially higher mean confidence than errors, confirming that the model’s logits provide a meaningful signal of choice accuracy.

4.1 Analysis of Phases 1 and 2 Performance, GPT4o

We next tested whether calibrated confidence predicts abstention behavior, as would be expected if it serves as a reliable metacognitive signal guiding decisions. In Phase 2, the model was exposed to the same multiple choice questions as in Phase 1, but had the additional option to abstain if they “didn’t see a clearly correct answer” (see Methods and Figure 1). Here performance was 30.0% correct, 13.4% incorrect, and 56.6% abstention. With the inclusion of an abstention option in Phase 2, correct responses increased from 63.9% to 69.1% consistent with a coverage-accuracy tradeoff (see Figure 7).

4.2 Phase 2: Computational Modeling (Logistic Regression), GPT4o

To determine whether this behavior reflects genuine metacognitive control – where internal confidence signals drive abstention decisions – we next turned to computational modeling. This allowed us to test whether abstention behavior in Phase 2 could be explained by a two-stage metacognitive framework (Figure 2). In this framework, Stage 1 represents the formation of an answer and associated confidence representation, while Stage 2 represents a threshold-based policy that maps confidence to abstention decisions. Critically, we used Phase 1 chosen confidence to model abstention behavior. In Phase 1, the model must select among real answer options without the possibility of abstaining, so the chosen confidence reflects the model’s internal evaluation of its selected response uncontaminated by the presence of an abstention option. Phase 1 confidence signals therefore provides a clean measure for testing whether confidence representations formed independently (Phase 1) generalize to drive abstention behavior when that option becomes available (Phase 2). Supporting the stability of these confidence representations, the Phase 1 chosen option remained the highest-confidence option among real alternatives in 82.0% of Phase 2 trials and 81.6% of Phase 4 trials, demonstrating substantial consistency in confidence ranking across phases despite the presence of the abstention option.

However, several alternative attributes aside from confidence could potentially guide abstention decisions. The model might rely on question difficulty—an objective measure of item hardness independent of the model’s subjective confidence on a particular trial. Abstention could also be driven by knowledge retrieval accessibility, measured through RAG scores that quantify how readily relevant information can be retrieved

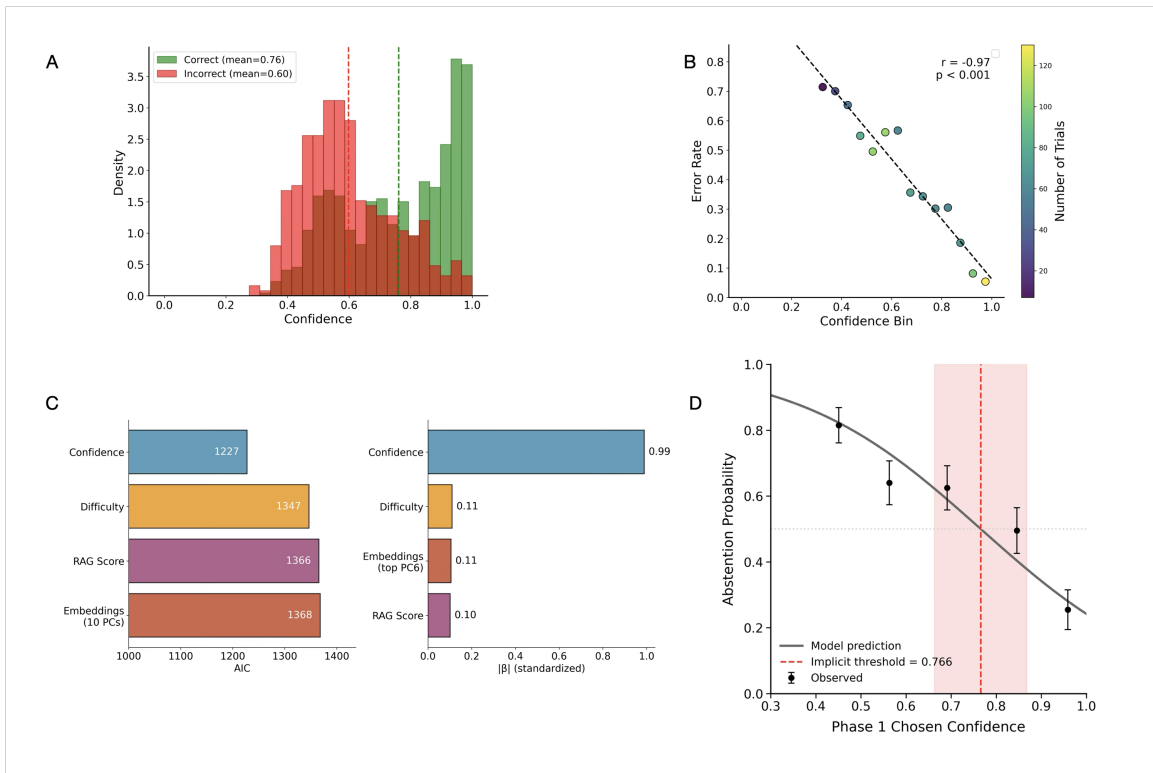


Figure 3: **GPT-4o confidence predicts error rate (Phase 1) and abstention behavior (Phase 2).** (A) Confidence distributions for correct (green) and incorrect (red) Phase 1 responses. Dashed vertical lines denote the mean confidence for each group. (B) Relationship between binned confidence and error rate in Phase 1. Each point represents a confidence bin (width = 0.05); color encodes the number of trials. A strong negative correlation was observed between confidence and error rate ($r = -0.97$, $p < 0.001$). Model was calibrated on a separate set of 1000 trials (see Methods). (C) Model comparison showing confidence as the dominant predictor of abstention. Left panel: AIC values for single-predictor models, where lower values indicate better fit. Right panel: Standardized effect sizes from the full model including all predictors. Confidence exhibits an effect size ($|\beta_{\text{std}}| = 0.99$) approximately 10 times larger than alternative predictors, demonstrating that abstention is driven by metacognitive confidence rather than question difficulty, knowledge accessibility, or surface-level semantic features. (D) Logistic regression model of natural abstention probability as a function of confidence for $n = 1000$ trials. The grey curve indicates the model prediction from the confidence + difficulty model, holding difficulty at its mean value. The red dashed line marks the implicit decision threshold at 77%, where $P(\text{abstain}) = 0.5$. The red shaded region denotes the confidence interval spanning approximately ± 10 percentage points around the threshold, illustrating the gradual transition of the decision boundary. Black circles represent observed abstention rates (mean \pm 95% CI) across confidence quintiles. Together, these panels reveal GPT-4o’s intrinsic abstention policy: higher internal confidence corresponds to a lower likelihood of abstaining, even without explicit threshold instructions.

from the model’s training corpus (see Methods)(Lewis et al., 2020). Additionally, surface-level linguistic features—captured through sentence embedding similarity scores—might signal when questions fall outside the model’s training distribution, potentially triggering abstention (Bommasani et al., 2021; Reimers and Gurevych, 2019).

To adjudicate among these possibilities, we used logistic regression to model binary abstention choices, quantifying the relative contribution of each potential driver while recovering the implicit threshold and

policy temperature parameters governing Stage 2 decisions if confidence emerges as the dominant factor (see Methods). To foreshadow the results, a logistic regression analysis revealed that Phase 1 chosen confidence was the dominant predictor of abstention decisions, substantially outperforming alternative mechanisms based on knowledge accessibility, surface-level semantic features, or aggregate question difficulty. Notably, the latter three measures were only relatively weakly correlated with one another (see Methods).

We first examined each potential predictor in isolation ($n = 1000$ trials, residual $df = 998$). Question difficulty—calculated as the mean accuracy across 20 independent runs of GPT-4o with different random seeds controlling answer position allocation (see Methods)—provided only modest predictive power (AIC = 1346.6, pseudo- $R^2 = 0.019$, $\beta_D = -1.03 \pm 0.20$, $z = -5.04$, $p < 0.001$)(Figure 3C, left panel). This multi-seed difficulty score represents the expected probability of correctness across random allocations—an item-level measure of intrinsic hardness (e.g., relating to question ambiguity, length, or topic complexity)—whereas the single-trial Phase 1 confidence reflects GPT-4o’s subjective certainty given a particular allocation. Notably, even under perfect calibration, these two quantities coincide only in expectation across seeds. Including difficulty as a covariate thus controls for objective item hardness while preserving the within-trial confidence signal that drives abstention.

In marked contrast, Phase 1 chosen confidence alone provided strikingly better fit (AIC = 1227.4, pseudo- $R^2 = 0.106$), reducing AIC by 119.2 points relative to difficulty. The confidence effect was substantial ($\beta_C = -4.87 \pm 0.47$, $z = -10.37$, $p < 0.001$), indicating that higher internal confidence strongly reduces the probability of abstention. Importantly, however, adding the model’s chosen confidence from Phase 1 to a model including difficulty markedly improved model fit (AIC = 1225.6, $\Delta\text{AIC} = -121.0$, pseudo- $R^2 = 0.109$, LR $\chi^2(1) = 123.02$, $p < 10^{-28}$). In the combined model, the effect of difficulty was marginal ($\beta_D = 0.50 \pm 0.26$, $z = 1.94$, $p = 0.053$), confirming that abstention behavior is driven primarily by GPT-4o’s internal confidence rather than by external question difficulty. In practical terms, a 0.1-unit increase in confidence (e.g., from 0.7 to 0.8) reduces the model’s probability of abstaining by approximately 12 percentage points.

To test whether alternative mechanisms beyond difficulty could account for abstention behavior, we additionally examined knowledge retrieval accessibility (RAG scores) and surface-level semantic features (sentence embeddings). RAG scores, which quantify knowledge retrieval accessibility by measuring semantic similarity between questions and retrieved passages from the model’s training corpus, performed poorly as a sole predictor of abstention (AIC = 1365.6, pseudo- $R^2 = 0.005$). Similarly, surface-level semantic features captured through sentence embeddings (represented as 10 principal components) showed limited predictive power (AIC = 1368.2, pseudo- $R^2 = 0.017$)(Figure 3C, left panel).

To directly test whether confidence provides explanatory power beyond alternative mechanisms, we conducted likelihood ratio tests comparing models with and without confidence. Adding confidence to a model already containing RAG scores produced a highly significant improvement (LR $\chi^2(1) = 141.13$, $p < 10^{-32}$, $\Delta\text{AIC} = -139.1$, $\Delta\text{pseudo-}R^2 = 0.103$). Similarly, adding confidence above embeddings yielded strong gains (LR $\chi^2(1) = 164.22$, $p < 10^{-37}$, $\Delta\text{AIC} = -162.2$, $\Delta\text{pseudo-}R^2 = 0.120$). Notably, the reverse tests revealed that neither RAG nor embeddings added substantial explanatory power once confidence was included: RAG above confidence produced only a non-significant very marginal improvement (LR $\chi^2(1) = 2.96$, $p = 0.085$, $\Delta\text{AIC} = -1.0$), while embeddings provided a modest but significant contribution (LR $\chi^2(10) = 41.42$, $p < 10^{-5}$, $\Delta\text{AIC} = -21.4$).

We next examined the full model including all predictors simultaneously to assess their relative contributions. To enable direct comparison of effect sizes, we standardized all continuous predictors (zero mean, unit variance). In this full model, confidence remained overwhelmingly dominant ($\beta_{\text{std}} = -0.989 \pm 0.094$, $z = -10.56$, $p < 10^{-25}$)(Figure 3C, right panel). The standardized effects of alternative predictors

were an order of magnitude smaller: RAG ($\beta_{\text{std}} = -0.102 \pm 0.075$, $z = -1.35$, $p = 0.178$), difficulty ($\beta_{\text{std}} = 0.110 \pm 0.086$, $z = 1.29$, $p = 0.197$), and the strongest embedding component (PC6: $\beta_{\text{std}} = 0.106 \pm 0.026$, $z = 4.04$, $p < 10^{-4}$). The confidence effect was 9.7 times larger than RAG, 9.0 times larger than difficulty, and 9.4 times larger than the top embedding component.

Using the unstandardized coefficients in the confidence-only model, we can recover the implicit decision parameters underlying GPT-4o’s abstention policy. Although an explicit abstention threshold was never specified in the Phase 2 instructions, the logistic form of our model allows us to infer an implicit decision threshold (see Methods). We found the confidence level at which the model abstains 50% of the time—the indifference point T_{50} —to be approximately 77% (for an average-difficulty question). The policy temperature parameter (20 confidence units) indicates a relatively gradual transition between answering and abstaining around this indifference point (see Figure 3D).

The finding that a 0.1-unit increase in confidence decreases abstention probability by roughly 12 percentage points underscores the strong coupling between GPT-4o’s internal confidence and its abstention behavior. Moreover, the smooth transition around the indifference point suggests that GPT-4o implements a soft, probabilistic thresholding policy—rather than an all-or-nothing rule—paralleling patterns of confidence-based decision-making observed in humans (i.e., Stage 2 in Figure 2; see Kepecs and Mainen, 2012). The inferred indifference point (i.e., 77% confidence) thus captures GPT-4o’s implicit criterion for acting on versus withholding a decision. The relatively high implicit threshold (77%) indicates that GPT-4o requires substantial confidence before choosing to answer in this context.

Critically, this pattern demonstrates that abstention is driven by metacognitive confidence representations rather than by proxies for knowledge accessibility (RAG scores), learned associations with question surface features (sentence embeddings), or aggregate difficulty estimates. In Phase 4, we directly manipulated this policy by instructing the model to abstain below explicit confidence thresholds, allowing a causal test of the link between confidence and abstention behavior. While our focus here is GPT-4o, similar qualitative behavior was observed in Gemma 3 27B, DeepSeek 671B and Qwen 80B (see Supplemental Results).

4.3 Phase 3: Activation Steering in Gemma 3 27B

The results from phase 2 provide evidence that internal signals of confidence drive LLM’s abstention behavior, with the model performing a metacognitive assessment – that is a comparison of its own confidence to an implicit threshold – resulting in a tendency to abstain or answer. We next sought more direct evidence that confidence influences abstention behavior, through a causal manipulation that intervenes at the level of confidence representations (i.e. Stage 1 of the confidence-decision pathway; see Figure 2). Specifically, we asked if the injection of neural activation patterns associated with high or low confidence states into the network at inference time would significantly influence the tendency of the model to abstain or answer (see Methods for details). Based on the tight coupling between (increases in) internal confidence and (decreases in) abstention rate, we hypothesized that if confidence causally drives abstention decisions, then artificially injecting neural activation patterns associated with high confidence states should reduce abstention rates, while injecting patterns associated with low confidence states should increase abstention rates.

To achieve this, we utilized the procedure of activation steering (see (Turner et al., 2023; Stolfo et al., 2024)), a process feasible in the Gemma 3 27B model (but not GPT4o). To isolate confidence representations that drive the answer-versus-abstain decision, we constructed steering vectors by contrasting trials based on the difference between the model’s confidence in its best answer option and its confidence in abstaining (i.e. the confidence margin; see Methods). We first derived steering vectors by contrasting neural activation patterns from 25 high confidence margin trials against 25 low confidence margin trials, matched for option

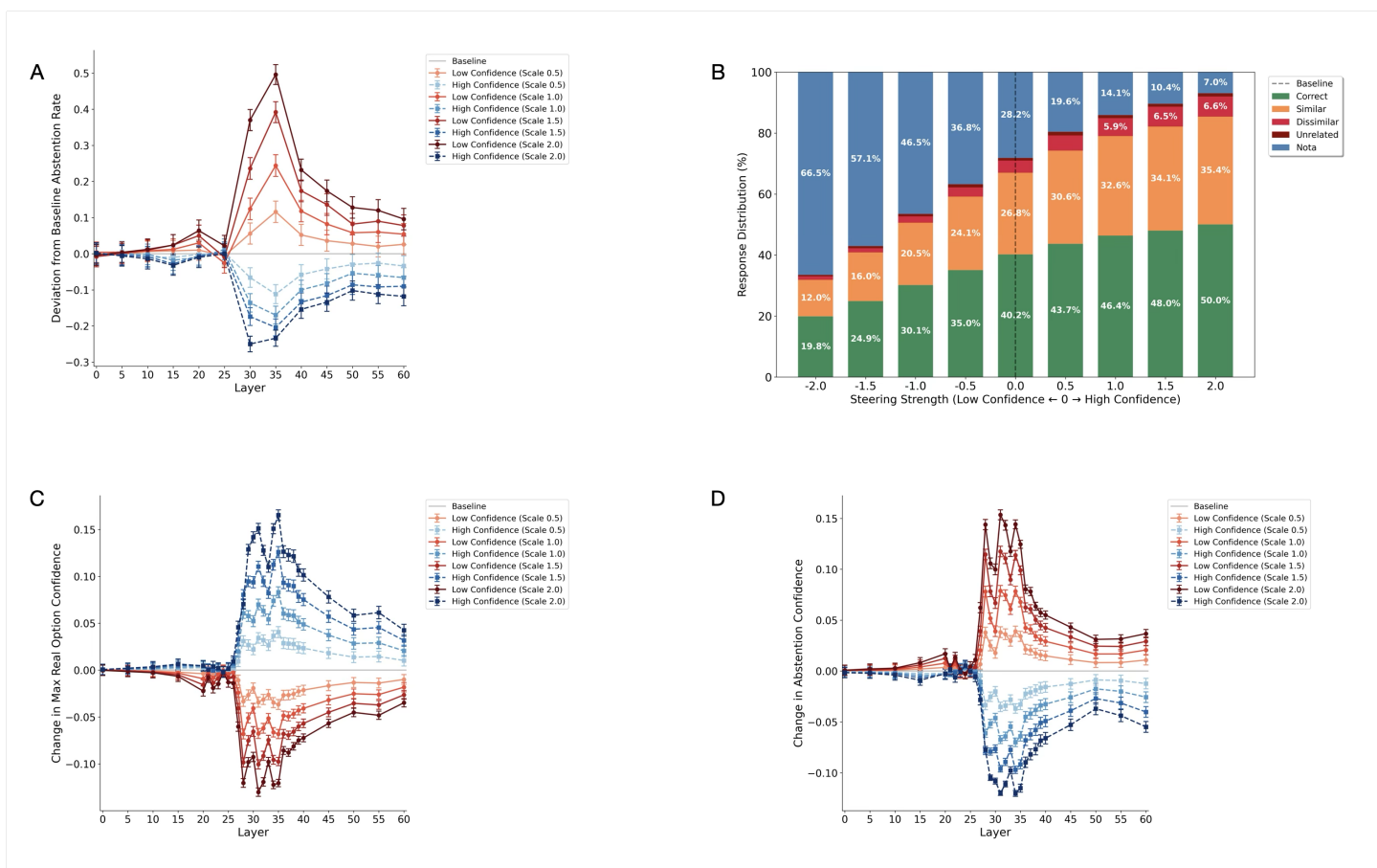


Figure 4: Effects of Activation Steering on Abstention Behavior and Confidence in Gemma 3 27B. (A) Change from baseline rate of abstention as a result of high and low confidence activation steering. Errors bars reflect SEM. Baseline level of abstention in no steering condition is 28.2%. (B) Response distribution averaged across layers 30-40 as a function of steering strength (from low confidence (negative), baseline (0), high confidence (positive)) (C) Change from baseline confidence – max of the real options (regardless of whether a real option or abstention was the outcome), and (D) Change from baseline confidence of abstention confidence (regardless of outcome), as a result of high and low confidence steering. Baseline max real confidence was 0.37, and abstention confidence was 0.25.

selection and accuracy (see Methods). Subtracting the mean low confidence activation from the mean high confidence yielded a single high-confidence steering vector (for each network layer), with the low-confidence vector being its inverse. At test time, we injected either the high or low confidence margin (hereafter, “high confidence” and “low confidence”) vector—scaled by a constant—at a specific layer in the network during inference on all 500 questions, such that processing in the rest of the model proceeded as normal (see Methods).

We observed that activation steering with high and low confidence vectors markedly influenced abstention behavior, reducing and increasing abstention rates, respectively—as hypothesized (see Figure 4A). The effect peaked in the mid-layers of the 62 layer network – specifically layer 31 (see Figure 8). The proportion of questions to which the model abstained declined from 66.5% at maximum low-confidence steering (steering strength = -2) to 7.0% at maximum high-confidence steering (steering strength = +2) – a 59.5 percentage point reduction representing 15.34% change per unit increase in steering strength ($r = -0.99$, $p < 0.001$; averaged across layers 30-40) (see Figure 4B).

We asked whether this marked change in abstention behavior was accompanied by underlying changes in confidence ratings induced by steering, compared to a baseline where no steering was used. We observed boosts (or reduction) in confidence due to high (or low) confidence vector steering – not only in relation to the maximum value of the confidence in the real options (regardless of answer/abstain decision – hereafter, termed maximum real confidence; see Figure 4C), but also in relation to confidence in the abstention option (see Figure 4D). Notably, the change in maximum real confidence was highly correlated with the change in the confidence in the abstention option ($r(43998) = -0.89$, $p < 0.001$, Cohen’s $d = 4.0$) – suggesting that steering influences abstention rates through a coordinated shift in confidence from the abstention option towards the real options.

Notably, activation steering produced a small but significant linear decrease in response accuracy (among answered questions) as steering strength increased from low confidence (-2) to high confidence ($+2$). Accuracy declined from 59.2% at maximum low-confidence steering to 53.7% at maximum high-confidence steering, representing a systematic decrease of 1.36% per unit increase in steering strength ($r = -0.94$, $p < 0.001$, $R^2 = 0.89$) (see Figure 4B) – consistent with a relatively mild coverage-accuracy tradeoff (i.e. change in coverage from 33.5% to 93%, corresponding to -2 and $+2$ steering strength, respectively).

4.3.1 Mediation analysis

Next, we investigated the key question of whether the effects of steering on abstention rate were actually *caused* by the influence of steering on confidence ratings, or alternatively, through changes in the decision policy that maps confidence to abstention choices – with the observed effects on confidence (Figure 4B and C) being incidental. To do this, we conducted a parallel mediation analysis, averaging across layers where the steering effect was prominent (layers 30-40 inclusive). Given the high correlation between change in maximum real confidence and change in abstention confidence (see Figure 4), we created a composite mediator – specifically, a confidence redistribution mediator—the net confidence shift from abstention toward real options, computed as: $(\Delta_{\max \text{ real}} - \Delta_{\text{abstention}})$ (see Methods for details). For example, if high-confidence steering increases max real confidence by $+0.10$ and decreases abstention confidence by -0.05 , the net redistribution is $+0.15$ toward answering. We also created an additional mediator – a policy shift mediator—capturing how steering alters the decision rule itself (thresholds and policy temperature) that maps confidence to abstention decisions. This was computed as the difference in predicted abstention probability for each trial between steered and baseline calibration curves, holding confidence constant (see Methods).

A parallel mediation analysis distinguishes between three pathways through which activation steering could reduce abstention behavior: two indirect pathways—one operating through confidence redistribution and another through changes in the decision policy—versus a direct pathway representing mechanisms outside these measured mediators (see Figure 5).

As expected, the mediation analysis revealed that activation steering significantly reduced abstention selection rates (total effect: $c = -0.824$, 95% CI $[-0.885, -0.673]$, $p < 0.001$). Critically, confidence redistribution was the dominant mechanism underlying the effect of steering on abstention rates (67.1% of the total effect; see Figure 5). High-confidence steering increased the net confidence shift toward real options ($a_1 = 0.107$, $p < 0.001$), which in turn strongly reduced abstention odds ($b_1 = -5.15$, $p < 0.001$), yielding an indirect effect of $a_1 \times b_1 = -0.55$ (95% CI $[-0.65, -0.47]$).

A secondary pathway operated through policy changes (26.2% of the total effect), with an indirect effect of $a_2 \times b_2 = -0.22$ (95% CI $[-0.24, -0.19]$). The total indirect effect across both pathways was -0.77 (95% CI $[-0.89, -0.67]$).

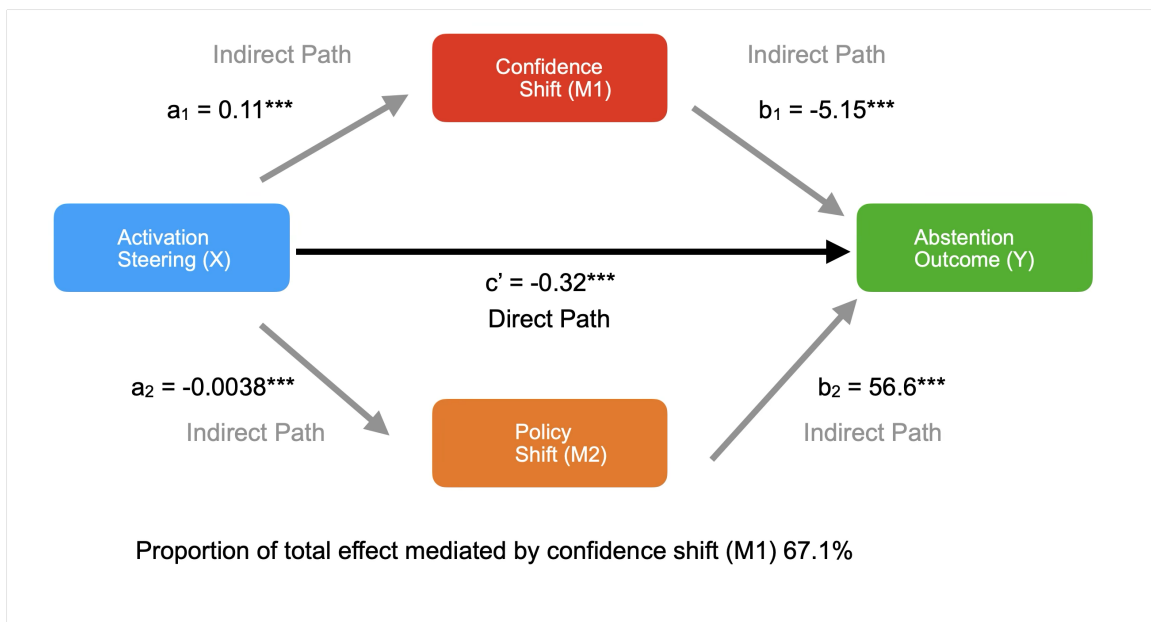


Figure 5: **Results of Gemma 3 27B parallel mediation analysis: confidence redistribution is the dominant mechanism underlying steering effects on abstention.** Path diagram showing how activation steering influences abstention rates through two parallel indirect pathways (confidence redistribution and policy changes) and a direct pathway. The confidence shift mediator (M_1) represents the change in maximum real confidence minus the change in abstention confidence induced by steering. The policy shift mediator (M_2) captures changes in the calibration curve mapping confidence to abstention probability. There was only a weak correlation between these mediators ($r = -0.24, p < 0.001$). Activation steering significantly increased net confidence shift toward real options ($a_1 = 0.11, p < 0.001$), which in turn strongly reduced abstention odds ($b_1 = -5.15, p < 0.001$), yielding an indirect effect of $a_1 \times b_1 = -0.55$ (95% CI [-0.65, -0.47]). Steering had a small but significant effect on the decision policy ($a_2 = -0.0038, p < 0.001$), and policy shifts exerted a strong effect on abstention when they occurred ($b_2 = 56.6, p < 0.001$), yielding an indirect effect of $a_2 \times b_2 = -0.22$ (95% CI [-0.24, -0.19]). A direct effect persisted after controlling for both mediators ($c' = -0.32, p < 0.001$), relative to a total effect of $c = -0.82$ ($p < 0.001$). Due to the nonlinear logit link function, the sum of the direct and indirect effects do not sum to the total effect, though the relative contributions remain interpretable. Confidence redistribution accounted for 67.1% of the total effect, while policy shifts accounted for 26.2%. All paths significant at $p < 0.001$ (***)).

A direct effect of $c' = -0.32$ (95% CI [-0.24, -0.09]) remained after accounting for both mediators. The combined proportion of the total effect mediated through both pathways (93.3%) indicates that the measured mediators account for most of the steering effect on abstention, with confidence redistribution being the primary mechanism. Note that due to the nonlinear logit link function, the sum of the direct and indirect effects do not sum to the total effect, though the relative contributions remain interpretable (VanderWeele, 2015).

These findings demonstrate that confidence steering operates primarily through a coherent confidence redistribution process: steering reallocates confidence from abstention toward concrete answer choices, with approximately two-thirds of the abstention reduction attributable to this reallocation mechanism (See Figure 5). The remaining indirect effect operates through changes in how confidence maps to decisions, confirming a two-stage model where steering affects both what the model believes about the correctness

of the option (Stage 1: confidence formation) and, to a lesser extent, how it uses those beliefs to decide (Stage 2: decision policy).

Our primary mediation analysis compared each item to itself under steered versus unsteered conditions, thereby controlling for stable item-level properties such as baseline difficulty or abstention rate (see Methods). However, this within-item approach does not rule out a subtler confound: item difficulty might influence how strongly steering affects confidence. If easier questions produce larger confidence shifts under steering—and also independently elicit fewer abstentions—then the apparent mediation by confidence could partly reflect a shared dependence on difficulty rather than a direct causal link from confidence to abstention.

To address this possibility, we re-ran the mediation analysis including an explicit *difficulty covariate*. We used multiseed-derived difficulty scores that estimate the probability of a correct answer across 20 random-seed model runs for each item (ranging from 0 = hard to 1 = easy; mean = 0.66, SD = 0.32). These GPT4o based difficulty scores provide an objective, model-agnostic measure of item difficulty that approximates the intrinsic solvability of each question.

When item difficulty was included as a covariate, the mediation pattern remained virtually unchanged. Activation steering continued to increase net confidence shift toward real options ($a = 0.11$, 95% CI [0.10, 0.11]), which in turn strongly reduced abstention odds ($b = -5.56$, 95% CI [-6.33, -4.86]), yielding an indirect effect of $a \times b = -0.60$ (95% CI [-0.69, -0.52]). The total effect of steering on abstention was $c = -0.84$, with a remaining direct effect of $c' = -0.30$ after accounting for the mediator. Item difficulty independently predicted lower abstention ($\gamma = -1.06$, $p < 0.001$), indicating that easier items generally elicited fewer abstentions. Crucially, after controlling for difficulty, the indirect effect via confidence redistribution remained strong and significant, accounting for 71.0% of the total effect.

In an additional analysis, we also verified that results were consistent when using a Gemma-specific difficulty score computed from Gemma’s own multiseed performance distribution, ensuring that the control reflects the model’s internal notion of difficulty (see Supplemental Results).

The results from Phase 3 demonstrate that intervening at the level of confidence signals has a robust effect on abstention behavior – and reveal the mechanistic underpinnings of this phenomenon. Specifically, the results of our mediation analyses demonstrate that activation steering has a specific effect in boosting/suppressing confidence signals (i.e. Stage 1; see Figure 2) – whilst leaving the thresholding and action-selection (i.e. Stage 2) process largely unchanged. Together, these findings provide compelling support for the hypothesis that confidence signals play a causal role in guiding behavior in LLMs.

4.4 Phase 4: Instructed Threshold, GPT4o Analysis of Performance

In the fourth phase, LLMs were instructed to abstain only when their confidence fell below a specified threshold, which we systematically varied. This manipulation, motivated in part by prior arguments for instructed thresholds to mitigate overconfident hallucinations (see (Kalai et al., 2025)), directly targets Stage 2 of the confidence–decision pathway – the thresholding and action-selection components – allowing us to test whether altering the policy causally influences abstention rates. Furthermore, this design tests whether threshold instructions operate purely at the decision boundary (Stage 2) or also influence the internal confidence representations themselves (Stage 1).

We first examined the overall pattern of correct, incorrect and abstention responses shown by the model (see Figure 6A). As expected, there was a clear effect of threshold on abstention rate—with increasing abstention rates as the threshold was increased. We next assessed whether the model’s accuracy increased

alongside increasing abstention rates (see Figure 9). A logistic regression revealed a significant positive effect of threshold on answer accuracy, such that higher thresholds led to more accurate responses among answered trials ($\beta = 0.0051 \pm 0.001$, $z = 3.97$, $p < 0.001$). This corresponds to roughly a +1.1% increase in accuracy for every 10% increase in threshold, consistent with the selective trade-off whereby stricter thresholds reduce coverage but improve the reliability of answers given.

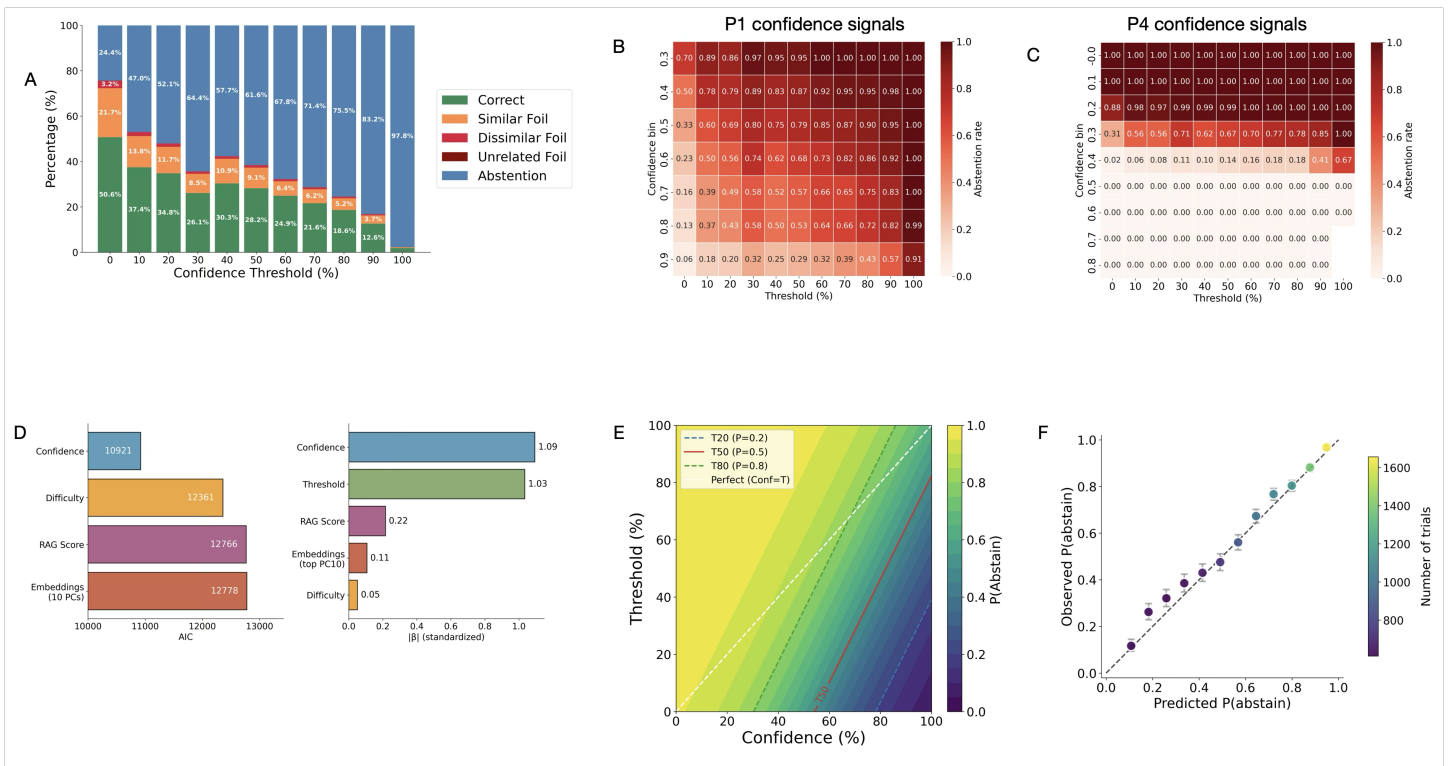


Figure 6: Phase 4: GPT-4o abstention behavior under explicit threshold instructions. (A) Profile of model responses across instructed confidence thresholds. Numbers inside bars reflect percentages. As threshold increases, abstention rate (blue) increases. (B) Abstention rate as a function of instructed threshold (x-axis) and model confidence (y-axis). When plotted against Phase 1 chosen confidence, abstention exhibits a diagonal gradient (bandness index = 0.042), consistent with Phase 1 confidence being pre-decisional—formed independently and then compared against threshold as separate inputs to the decision rule (see Supplemental text for details). (C) Abstention rate as a function of instructed threshold (x-axis) and model confidence (y-axis). When plotted against Phase 4 confidence (maximum value among real options), abstention collapses into horizontal bands (bandness index = 0.78) determined almost entirely by confidence, with threshold having little independent effect. This pattern demonstrates that Phase 4 confidence is post-decisional—it reflects the output of the threshold-conditioned abstention policy rather than the upstream belief signal (see Supplemental text for details). (D) Model comparison showing confidence as the dominant predictor of abstention. Left panel: AIC values for models with threshold plus single additional predictor, where lower values indicate better fit. Confidence substantially outperforms difficulty, RAG score, and sentence embeddings. Right panel: Standardized effect sizes from the full model including all predictors simultaneously. Confidence and threshold exhibit comparable effect sizes, both substantially larger than alternative predictors: RAG, difficulty, and top embedding component. (E) Computational model of the decision rule governing abstention. Behavior of a perfectly calibrated model is shown along the diagonal (i.e., Confidence = Threshold). In comparison, the fitted model (confidence + threshold + difficulty) exhibits conservatism driven by a large negative baseline bias (shift = -97.6%), but this is partially offset by substantial overweighing of internal confidence (scale = 1.80). For example, at 80% confidence, the model’s indifference point occurs at threshold $\approx 46\%$, meaning it abstains 50% of the time despite its confidence substantially exceeding the threshold. The steep slope of the contours (e.g., T_{50}) reflects this overweighing: a 1% increase in confidence offsets approximately 1.80% of instructed threshold. Contours T_{20} , T_{50} , T_{80} mark thresholds at which the model abstains with 20%, 50%, 80% probability. Points to the right/below each line correspond to lower abstention rates, while points to the left/above correspond to higher abstention rates. The relatively wide gap between T_{20} and T_{80} reflects the soft transition (policy temperature = 31.0 in percent units) of the decision boundary. (F) Illustration of abstention model fit. Observed versus predicted abstention rates in 12 bins. Error bars: 95% Wilson confidence intervals. Color indicates bin size. Dashed line: perfect calibration.

We next examined whether abstention behavior was systematically shaped by the instructed threshold, and whether this influence was modulated by the model’s own confidence (Figure 6B). Within our two-stage framework, confidence representations are formed at Stage 1, then subsequently used at Stage 2 where they are compared against a threshold via the decision policy $\sigma((T - C)/\tau)$. An important methodological choice was to use Phase 1 confidence estimates as predictors of Phase 4 behavior. Phase 1 confidence represents a pre-decisional measure—the model’s confidence in its answer extracted when no abstention option exists. In contrast, Phase 4 confidence is post-decisional: because the model has been instructed to apply a threshold, its confidence estimates have already incorporated the threshold comparison rather than representing the raw belief signal. As we show below, this distinction is borne out empirically in the structure of abstention behavior.

We examined abstention rate as a joint function of threshold and confidence. When plotted against Phase 1 confidence, abstention exhibits a smooth diagonal gradient (Figure 6B), consistent with threshold and confidence acting as independent inputs where a pre-decisional confidence signal is compared against the threshold. In marked contrast, when plotted against Phase 4 confidence, abstention collapses into horizontal bands (Figure 6C), indicating that Phase 4 confidence has already incorporated the threshold instruction and reflects post-decisional processing (see Supplemental text for details).

Having established that Phase 1 confidence captures pre-decisional Stage 1 representations, we can now use it as a probe to determine whether instructed thresholds operate at Stage 1 (confidence formation) or Stage 2 (decision policy). Specifically, if Phase 1 confidence signals maintains their predictive power, this indicates thresholds operate primarily at Stage 2 (altering the decision policy) while leaving Stage 1 confidence representations fundamentally unchanged. Conversely, if Phase 1 confidence signals lose their predictive power, it would suggest threshold instructions alter confidence processing from the ground up, fundamentally changing Stage 1 representations themselves.

4.5 Phase 4: Computational Modeling of Abstention Data under Instructed Thresholds, GPT4o

We fit a quantitative model to the profile of abstention behavior observed. Specifically, we asked whether chosen confidence from Phase 1 was a robust predictor of abstention behavior, above and beyond any effects of instructed threshold and difficulty. As in Phase 2, we also tested whether alternative mechanisms—knowledge retrieval accessibility (RAG scores) and surface-level semantic features (sentence embeddings)—could account for abstention patterns beyond confidence and threshold. To do this, we set up nested logistic regression models whose dependent variable was binary abstention decisions, and included predictors for chosen confidence, instructed threshold, question difficulty, RAG scores, and sentence embeddings (see Methods).

To test whether models use confidence to implement instructed thresholds, we compared regression models predicting abstention from different predictor sets (see Table 3 and Figure 6D). A model including confidence and threshold ($n = 11000$, residual $df = 10997$) dramatically outperformed a threshold-only baseline ($\Delta AIC = -1953$, likelihood ratio $\chi^2(1) = 1955$, $p < 0.001$), more than doubling explained variance (pseudo- R^2 : $0.11 \rightarrow 0.24$). Alternative predictors fared far worse: adding RAG scores or sentence embeddings to threshold produced negligible improvement over threshold alone, and adding these predictors to a threshold-plus-confidence model yielded only modest gains ($\Delta AIC \approx -50$), dwarfed by confidence’s contribution. Question difficulty, though statistically significant when added to the confidence model ($p = 0.025$), improved fit by less than 0.1% ($\Delta \text{pseudo-}R^2 = 0.001$)—confirming that difficulty has negligible practical importance once confidence is accounted for.

To assess relative contributions, we examined standardized effect sizes from the full model including all predictors (Figure 6D right panel). Confidence ($\beta_{\text{std}} = -1.09 \pm 0.03$, $z = -34.1$, $p < 10^{-254}$) and threshold ($\beta_{\text{std}} = 1.03 \pm 0.03$, $z = 38.4$, $p < 10^{-320}$) exhibited comparable effect sizes, both substantially larger than alternative predictors: RAG ($\beta_{\text{std}} = -0.22 \pm 0.03$, $z = -8.5$, $p < 10^{-16}$), difficulty ($\beta_{\text{std}} = 0.05 \pm 0.03$, $z = 1.8$, $p = 0.071$), and the strongest embedding component (PC10: $\beta_{\text{std}} = -0.11 \pm 0.02$, $z = -4.5$, $p < 10^{-5}$). The confidence effect was 5.1 times larger than RAG, 21.3 times larger than difficulty, and 10.2 times larger than the top embedding component. These results confirm that Phase 1 confidence retains its predictive power even when thresholds are experimentally manipulated, and that abstention is driven by confidence rather than by knowledge accessibility, surface features, or aggregate difficulty. This supports the operational independence of Stage 1 (confidence formation) and Stage 2 (threshold-based policy): instructed thresholds alter how confidence is used without changing the confidence representations themselves.

We next examined the fitted coefficients from the confidence plus threshold plus difficulty model to understand how the model integrates confidence and threshold information. As expected, abstention rate increased with threshold ($\beta_T = 0.033$, SE=0.001, $z = 38.4$, $p < 0.001$) and decreased with confidence ($\beta_C = -0.058$, SE=0.002, $z = -34.1$, $p < 0.001$). Difficulty was marginal ($\beta_D = 0.159$, SE=0.088, $z = 1.8$, $p = 0.071$) (see Table 2).

From these coefficients, we derived three interpretable decision parameters (see Methods): scale (1.80), which quantifies how much the model weights its internal confidence relative to the instructed threshold; shift (-97.6), which captures baseline abstention bias; and policy temperature (31.0), which measures the softness of the decision boundary. Notably, the scale parameter of 1.80 reveals that GPT-4o weights its internal confidence signals nearly twice as heavily as the instructed thresholds. In practical terms, a 1% increase in the model’s own confidence offsets approximately 1.80% of instructed threshold.

We also computed the indifference threshold, T_{50} , at which the model is equally likely to answer or abstain: for example, at a confidence level of 80% the model’s indifference point is a threshold of approximately 46% (see Figure 6E). Under symmetric costs (i.e. a wrong answer and an abstention response are equally bad), a perfectly calibrated model would abstain whenever its confidence falls below the instructed threshold. The negative baseline bias (-97.6%) shifts the decision boundary downward, causing the model to abstain at confidence levels above threshold—a pattern consistent with treating errors as costlier than unnecessary abstentions. This conservatism is partially offset by the model’s overweighting of its own confidence signals (scale = 1.80), which steepens the decision boundary. However, even this elevated confidence weighting does not fully compensate for the baseline bias: at maximum confidence (100%), the model’s indifference point remains at approximately 80%, indicating persistent conservatism across the full confidence range. Despite these asymmetric tendencies, the two-stage logistic model accurately captured the relationship between confidence, threshold, and abstention, with predicted abstention rates closely tracking observed rates across the full range of conditions (Figure 6F).

Phase 4 demonstrates that abstention behavior in GPT-4o is well captured by a quantitative model in which abstention probability is a joint function of internal confidence representations (Stage 1) and thresholding policies (Stage 2)(see Figure 6E). Notably, the strong predictive power of Phase 1 confidence—measured in the absence of threshold instructions—across all Phase 4 threshold conditions indicates that instructed thresholds operate primarily at Stage 2 (thresholding policy) rather than by fundamentally distorting Stage 1 confidence representations. However, the systematic overweighting of confidence signals (i.e. scale = 1.80) suggests that threshold instructions influence how confidence is weighted in decisions—though we can’t exclude secondary effects on Stage 1 processing whereby threshold instructions subtly alter confidence representations themselves beyond the primary Stage 2 thresholding mechanism.

Whilst our primary aim was to characterize the relationship between instructed thresholds, Phase 1 confidence and abstention behavior, for completeness we also analyzed the relationship between these predictors and the underlying driver of abstention behavior: a continuous variable, Phase 4 confidence in the abstention choice (see Figure 10). Our analyses of abstention confidence demonstrate that instructed threshold shifts the model toward abstention even before the decision boundary is crossed, while confidence pulls it back toward answering — providing convergent evidence, via a richer signal, for the same underlying mechanism identified in the binary analyses.

We also tested Gemma 3 27B, DeepSeek 671B and Qwen 80B on Phase 4 of the task. Of note, the prompt used with GPT-4o, DeepSeek and Qwen elicited few abstentions in Gemma 3 27B (see Methods and Supplemental Results for details), consistent with evidence that different models abstain to different extents (Wen et al., 2024, 2025), and model-specific differences in instruction adherence (Sclar et al., 2023). We therefore used a rephrasing of the basic prompt to ensure meaningful engagement of Gemma 3 27B with the abstention paradigm (see Methods for details of the prompt and the generation procedure). This approach allowed us to demonstrate that confidence signals similarly governed abstention once the behavior of interest – abstention – was elicited (see Supplemental Results).

5 Discussion

Our findings provide convergent evidence that LLMs exhibit metacognitive control, through leveraging confidence signals to guide abstention decisions. We observed signatures of a two-stage confidence–decision pathway across the phases of our experimental paradigm. In Phase 2, we found that the behavior of LLMs was consistent with the application of an implicit threshold to internal confidence estimates. Critically, confidence alone provided substantially better fit to abstention behavior than alternative mechanisms based on knowledge retrieval accessibility (RAG scores), surface-level semantic features (sentence embeddings), or aggregate question difficulty, with standardized effect sizes approximately an order of magnitude larger. In Phase 3, activation steering was used to directly intervene at the level of Stage 1 confidence signals, and thereby demonstrate the causal role of confidence signals in mediating abstention behavior. Finally, in Phase 4, we experimentally manipulated the threshold used by the model, allowing us to formalize how thresholding policies and confidence interact to shape abstention behavior. Taken together, these results demonstrate that abstention arises from the joint operation of confidence representations (Stage 1) and threshold-based policies (Stage 2), providing a computational account of how LLMs determine when to answer versus abstain.

We leveraged a two-stage confidence-decision framework to characterize the mechanistic basis of confidence-guided abstention decisions in LLMs, drawing inspiration from research in human neuroscience and psychophysics. This framework operates at a computational level of analysis, describing the functional architecture of how confidence guides meta-decisions without making claims about specific implementation in neural networks or transformer architectures. The framework builds on work demonstrating that human and non-human metacognitive decisions involve separable stages: confidence formation (Stage 1) and threshold-based action selection (Stage 2) (Fleming and Daw, 2017; Kepecs and Mainen, 2012)(see Figure 2). The Stage 1 component draws from research showing that confidence signals arise from the same evidence accumulation processes that drive primary decisions, while Stage 2 reflects threshold mechanisms identified in perceptual decision-making (see (Gold and Shadlen, 2007; Yeung and Summerfield, 2012; Pouget et al., 2016; Kiani and Shadlen, 2009)). However, whereas classic two-stage models describe how confidence emerges from evidence accumulation, our framework takes confidence representations as already formed and focuses on how they are deployed to guide meta-decisions. By applying this established framework to LLMs, we demonstrate that artificial systems exhibit strikingly similar architectural principles

for confidence-guided behavior, suggesting that the computational demands of metacognitive control may impose convergent solutions across biological and artificial intelligence systems.

Our abstention paradigm has striking parallels with post-decision wagering paradigms in psychophysics and neuroscience (Lak et al., 2014; Kepecs et al., 2008). In both scenarios, the agent must first make a primary decision – about the correct option in a multiple choice question, or the dominant chemical in an odor categorization task (Lak et al., 2014). They are then required to make a meta-decision – whether to answer or to abstain in the case of an LLM, or whether to wait for a reward or initiate a new trial in the case of a laboratory rat. Critically, this meta-decision – which involves a tradeoff between potential rewards and costs (e.g. the cost of making an error, compared to that of abstaining) – depends on the use of internal confidence signals relating to the primary decision, a continuous measure that must be translated into a binary outcome. Thus, our paradigm grounds LLM abstention within the same class of meta-decision processes long studied in psychophysics and neuroscience, providing a bridge between artificial and biological systems.

We performed two complementary causal interventions targeted each stage of the confidence-decision pathway. Activation steering has emerged as a powerful interpretability technique for causally manipulating internal model representations (Turner et al., 2023; Panickssery et al., 2023; Stolfo et al., 2024), yet to our knowledge has not been applied to investigate the role of confidence in guiding behavior. Our steering intervention provides direct causal evidence that confidence signals drive abstention: injecting high-confidence activation patterns reduced abstention rates, while low-confidence patterns increased them. Mediation analysis revealed that confidence redistribution—the reallocation of probability mass from abstention toward answer options—was the dominant mechanism, accounting for 67% of the total steering effect, with policy shifts contributing a further 26% —confirming that activation steering operates predominantly, though not exclusively, through Stage 1 confidence representations. A residual direct effect persisted after accounting for both mediators, possibly reflecting nonlinear interactions between confidence dimensions or dynamic changes in confidence during the decision process that our parallel mediator model does not capture. The observation that peak steering effects occurred at intermediate transformer layers suggests that confidence is encoded as a latent internal variable upstream of the final output logits—consistent with first-order accounts in which confidence derives from internal evidence signals used for the primary decision (Kepecs and Mainen, 2012; Kiani and Shadlen, 2009). However, this does not rule out higher-order monitoring at later stages (Fleming and Daw, 2017), and characterizing the precise computational architecture of confidence generation in LLMs remains an important direction for future work.

Our second intervention provided direct causal evidence that threshold policies control abstention behavior. Systematic manipulation of instructed thresholds in Phase 4 demonstrated that Stage 2 policies directly modulate abstention rates while leaving underlying confidence representations fundamentally unchanged—Stage 1 confidence retained its predictive power across all threshold conditions.

We observed substantial variation in abstention behavior across models, both in baseline propensity and in how models weighted confidence relative to instructed thresholds. In Phase 2 free abstention, baseline rates ranged widely: DeepSeek (82.0%), GPT-4o (56.6%), Qwen 80B (43.8%), and Gemma 3 27B (27.2%). In Phase 4, models differed in their baseline bias (the shift parameter), which quantifies the tendency to abstain independently of confidence or threshold. GPT-4o and Qwen 80B showed strong conservatism (shifts of -97.6% and -52.3% , respectively), while DeepSeek (-8.5%) and Gemma 3 27B ($+1.0\%$) showed minimal bias. Models also differed in how steeply confidence influenced their decisions relative to instructed thresholds (the scale parameter). Under symmetric costs and perfect calibration, $\text{scale} = 1.0$ represents a benchmark where the model treats its confidence and the instructed threshold as commensurate. GPT-4o and Qwen 80B exceeded this benchmark (scales of 1.80 and 1.49), producing steeper decision boundaries,

while Gemma 3 27B fell below it (scale = 0.66), yielding flatter boundaries. Only DeepSeek approximated the benchmark (scale = 1.05). These systematic deviations likely reflect some combination of implicit cost asymmetries—where errors are weighted differently from unnecessary abstentions—and miscalibration of internal confidence signals. Disentangling these contributions remains an open question. Crucially, however, despite this quantitative variation, the fundamental two-stage architecture was preserved across all models: confidence robustly predicted abstention in every case. This dissociation—between variation in decision parameters and preserved computational structure—suggests that while training procedures shape the specifics of abstention policy, the use of confidence signals to guide metacognitive control emerges as a convergent solution across LLM implementations.

Prior work has largely implemented abstention as a thresholding process on confidence or uncertainty estimates, using either external calibrators or supervised constructs (Kirichenko et al., 2025; Tjandra et al., 2024; Chuang et al., 2024; Yadkori et al., 2024; Zhang et al., 2024). For example, Tjandra et al. (2024) compute semantic entropy during fine-tuning to provide abstention supervision, while Yadkori et al. (2024) employ conformal abstention based on post-hoc evaluation and self-consistency across samples. Chuang et al. (2024) introduce Self-REF, a fine-tuning framework that equips models with explicit confidence tokens via external supervision. Such paradigms do not examine native abstention dynamics, leaving open whether models use internal confidence signals or simply pattern-match to features correlated with training supervision or surface-level question properties (Wen et al., 2025). In our experiment, all questions were objectively answerable, and we explicitly tested and ruled out these alternative accounts: aggregate question difficulty, knowledge retrieval accessibility, and surface-level semantic features all provided substantially weaker predictions of abstention than internal confidence, with standardized effect sizes an order of magnitude smaller. Moreover, causal interventions targeting both confidence representations (activation steering) and decision thresholds (instructed threshold manipulation) systematically modulated abstention behavior—providing direct evidence that abstention is governed by intrinsic confidence dynamics within a two-stage confidence–decision pathway. These findings complement recent correlational evidence that internal confidence predicts subsequent behavior such as change of mind (Kumaran et al., 2025), establishing that confidence signals both predict and causally drive decision policies in LLMs.

Our findings provide causal evidence that LLMs exercise metacognitive control over abstention, using internal confidence signals to determine when to answer versus withhold responses. While prior research has demonstrated that confidence estimates can be extracted from LLM outputs and calibrated externally (Xiong et al., 2023; Tian et al., 2023; Steyvers et al., 2025; Tao et al., 2025; Kadavath et al., 2022) (e.g. using temperature scaling), our work establishes that models internally utilize these (uncalibrated) confidence signals to guide their own decisions—actively deploying them to control behavior. Notably, verbal confidence reports from LLMs are often markedly overconfident and poorly calibrated (Steyvers et al., 2025; Griot et al., 2025), yet our results show that models adaptively deploy internal confidence signals to guide behavior—suggesting a dissociation between metacognitive control and verbal introspection. Through systematic behavioral analysis, activation-steering interventions, and computational modeling, we demonstrate that LLMs generate, weight, and strategically deploy internal confidence signals within a two-stage framework that mirrors the computational architecture of biological metacognition. While recent work has reported introspective capacities in frontier models—the ability to access and report internal representational content (Anthropic, 2025)—our work establishes a capacity for metacognitive control: the use of internal evaluations of decision correctness to regulate behavior. An important direction for future research is to investigate the relationship between these introspective and control capacities, and how both emerge across different architectures, training procedures, and scales.

References

- Anthropic. Emergent introspective awareness in large language models. <https://transformer-circuits.pub/2025/introspection/>, 2025. Anthropic Research Report.
- Andy Arditi, Oscar Obeso, Aaquib Syed, Daniel Paleka, Nina Panickssery, Wes Gurnee, and Neel Nanda. Refusal in language models is mediated by a single direction. *Advances in Neural Information Processing Systems*, 37:136037–136083, 2024.
- Rishi Bommasani, Drew A Hudson, Ehsan Adeli, Russ Altman, Simran Arora, Sydney von Arx, Michael S Bernstein, Jeannette Bohg, Antoine Bosselut, Emma Brunskill, et al. On the opportunities and risks of foundation models. *arXiv preprint arXiv:2108.07258*, 2021.
- Yu-Neng Chuang, Prathusha Kameswara Sarma, Parikshit Gopalan, John Boccio, Sara Bolouki, Xia Hu, and Helen Zhou. Learning to route llms with confidence tokens. *arXiv preprint arXiv:2410.13284*, 2024.
- Kawin Ethayarajh. How contextual are contextualized word representations? comparing the geometry of BERT, ELMo, and GPT-2 embeddings. In *Proceedings of the 2019 Conference on Empirical Methods in Natural Language Processing and the 9th International Joint Conference on Natural Language Processing (EMNLP-IJCNLP)*, pages 55–65, 2019.
- Stephen M Fleming and Nathaniel D Daw. Self-evaluation of decision-making: A general bayesian framework for metacognitive computation. *Psychological review*, 124(1):91, 2017.
- Allison L Foote and Jonathon D Crystal. Metacognition in the rat. *Current Biology*, 17(6):551–555, 2007.
- Joshua I Gold and Michael N Shadlen. The neural basis of decision making. *Annu. Rev. Neurosci.*, 30(1):535–574, 2007.
- Maxime Griot, Coralie Hemptinne, Jean Vanderdonckt, and Demet Yuksel. Large language models lack essential metacognition for reliable medical reasoning. *Nature communications*, 16(1):642, 2025.
- Chuan Guo, Geoff Pleiss, Yu Sun, and Kilian Q Weinberger. On calibration of modern neural networks. In *International conference on machine learning*, pages 1321–1330. PMLR, 2017.
- Tim Tian Hua, Andrew Qin, Samuel Marks, and Neel Nanda. Steering evaluation-aware language models to act like they are deployed. *arXiv preprint arXiv:2510.20487*, 2025.
- Ian T Jolliffe and Jorge Cadima. Principal component analysis: a review and recent developments. *Philosophical Transactions of the Royal Society A: Mathematical, Physical and Engineering Sciences*, 374(2065):20150202, 2016.
- Saurav Kadavath, Tom Conerly, Amanda Askell, Tom Henighan, Dawn Drain, Ethan Perez, Nicholas Schiefer, Zac Hatfield-Dodds, Nova DasSarma, Eli Tran-Johnson, et al. Language models (mostly) know what they know. *arXiv preprint arXiv:2207.05221*, 2022.
- Adam Tauman Kalai, Ofir Nachum, Santosh S Vempala, and Edwin Zhang. Why language models hallucinate. *arXiv preprint arXiv:2509.04664*, 2025.
- Adam Kepecs and Zachary F Mainen. A computational framework for the study of confidence in humans and animals. *Philosophical Transactions of the Royal Society B: Biological Sciences*, 367(1594):1322–1337, 2012.
- Adam Kepecs, Naoshige Uchida, Hatim A Zariwala, and Zachary F Mainen. Neural correlates, computation and behavioural impact of decision confidence. *Nature*, 455(7210):227–231, 2008.

- Roозbeh Kiani and Michael N Shadlen. Representation of confidence associated with a decision by neurons in the parietal cortex. *science*, 324(5928):759–764, 2009.
- Polina Kirichenko, Mark Ibrahim, Kamalika Chaudhuri, and Samuel J Bell. Abstentionbench: Reasoning llms fail on unanswerable questions. *arXiv preprint arXiv:2506.09038*, 2025.
- Dharshan Kumaran, Stephen M Fleming, Larisa Markeeva, Joe Heyward, Andrea Banino, Mrinal Mathur, Razvan Pascanu, Simon Osindero, Benedetto De Martino, Petar Velickovic, et al. How overconfidence in initial choices and underconfidence under criticism modulate change of mind in large language models. *arXiv preprint arXiv:2507.03120*, 2025.
- Armin Lak, Gil M Costa, Erin Romberg, Alexei A Koulakov, Zachary F Mainen, and Adam Kepecs. Orbitofrontal cortex is required for optimal waiting based on decision confidence. *Neuron*, 84(1):190–201, 2014.
- Patrick Lewis, Ethan Perez, Aleksandra Piktus, Fabio Petroni, Vladimir Karpukhin, Naman Goyal, Heinrich Küttler, Mike Lewis, Wen-tau Yih, Tim Rocktäschel, et al. Retrieval-augmented generation for knowledge-intensive NLP tasks. In *Advances in Neural Information Processing Systems*, volume 33, pages 9459–9474, 2020.
- Nishanth Madhusudhan, Sathwik Tejaswi Madhusudhan, Vikas Yadav, and Masoud Hashemi. Do llms know when to not answer? investigating abstention abilities of large language models. *arXiv preprint arXiv:2407.16221*, 2024.
- Nina Panickssery, Nick Gabrieli, Julian Schulz, Meg Tong, Evan Hubinger, and Alexander Matt Turner. Steering llama 2 via contrastive activation addition. *arXiv preprint arXiv:2312.06681*, 2023.
- Benjamin Plaut, Nguyen X Khanh, and Tu Trinh. Probabilities of chat llms are miscalibrated but still predict correctness on multiple-choice q&a. *arXiv preprint arXiv:2402.13213*, 2024.
- Alexandre Pouget, Jan Drugowitsch, and Adam Kepecs. Confidence and certainty: distinct probabilistic quantities for different goals. *Nature neuroscience*, 19(3):366–374, 2016.
- Nils Reimers and Iryna Gurevych. Sentence-BERT: Sentence embeddings using Siamese BERT-networks. In *Proceedings of the 2019 Conference on Empirical Methods in Natural Language Processing and the 9th International Joint Conference on Natural Language Processing (EMNLP-IJCNLP)*, pages 3982–3992, 2019.
- Melanie Sclar, Yejin Choi, Yulia Tsvetkov, and Alane Suhr. Quantifying language models’ sensitivity to spurious features in prompt design or: How i learned to start worrying about prompt formatting. *arXiv preprint arXiv:2310.11324*, 2023.
- Mark Steyvers and Megan AK Peters. Metacognition and uncertainty communication in humans and large language models. *Current Directions in Psychological Science*, page 09637214251391158, 2025.
- Mark Steyvers, Heliodoro Tejada, Aakriti Kumar, Catarina Belem, Sheer Karny, Xinyue Hu, Lukas W Mayer, and Padhraic Smyth. What large language models know and what people think they know. *Nature Machine Intelligence*, pages 1–11, 2025.
- Alessandro Stolfo, Vidhisha Balachandran, Safoora Yousefi, Eric Horvitz, and Besmira Nushi. Improving instruction-following in language models through activation steering. *arXiv preprint arXiv:2410.12877*, 2024.

- Caleb Stone, Jason B Mattingley, and Dragan Rangelov. On second thoughts: changes of mind in decision-making. *Trends in Cognitive Sciences*, 26(5):419–431, 2022.
- Linwei Tao, Yi-Fan Yeh, Minjing Dong, Tao Huang, Philip Torr, and Chang Xu. Revisiting uncertainty estimation and calibration of large language models. *arXiv preprint arXiv:2505.23854*, 2025.
- Katherine Tian, Eric Mitchell, Allan Zhou, Archit Sharma, Rafael Rafailov, Huaxiu Yao, Chelsea Finn, and Christopher D Manning. Just ask for calibration: Strategies for eliciting calibrated confidence scores from language models fine-tuned with human feedback. *arXiv preprint arXiv:2305.14975*, 2023.
- Benedict Aaron Tjandra, Muhammed Razzak, Jannik Kossen, Kunal Handa, and Yarin Gal. Fine-tuning large language models to appropriately abstain with semantic entropy. *arXiv preprint arXiv:2410.17234*, 2024.
- Christian Tomani, Kamalika Chaudhuri, Ivan Evtimov, Daniel Cremers, and Mark Ibrahim. Uncertainty-based abstention in llms improves safety and reduces hallucinations. *arXiv preprint arXiv:2404.10960*, 2024.
- Alexander Matt Turner, Lisa Thiergart, Gavin Leech, David Udell, Juan J Vazquez, Ulisse Mini, and Monte MacDiarmid. Steering language models with activation engineering. *arXiv preprint arXiv:2308.10248*, 2023.
- Tyler VanderWeele. *Explanation in causal inference: methods for mediation and interaction*. Oxford University Press, 2015.
- Taylor W Webb, Kiyofumi Miyoshi, Tsz Yan So, Sivananda Rajananda, and Hakwan Lau. Natural statistics support a rational account of confidence biases. *Nature Communications*, 14(1):3992, 2023.
- Jason Wei, Nguyen Karina, Hyung Won Chung, Yunxin Joy Jiao, Spencer Papay, Amelia Glaese, John Schulman, and William Fedus. Measuring short-form factuality in large language models. *arXiv preprint arXiv:2411.04368*, 2024.
- Bingbing Wen, Bill Howe, and Lucy Lu Wang. Characterizing llm abstention behavior in science qa with context perturbations. *arXiv preprint arXiv:2404.12452*, 2024.
- Bingbing Wen, Jihan Yao, Shangbin Feng, Chenjun Xu, Yulia Tsvetkov, Bill Howe, and Lucy Lu Wang. Know your limits: A survey of abstention in large language models. *Transactions of the Association for Computational Linguistics*, 13:529–556, 2025.
- Miao Xiong, Zhiyuan Hu, Xinyang Lu, Yifei Li, Jie Fu, Junxian He, and Bryan Hooi. Can llms express their uncertainty? an empirical evaluation of confidence elicitation in llms. *arXiv preprint arXiv:2306.13063*, 2023.
- Yasin Abbasi Yadkori, Ilja Kuzborskij, David Stutz, András György, Adam Fisch, Arnaud Doucet, Iuliya Beloshapka, Wei-Hung Weng, Yao-Yuan Yang, Csaba Szepesvári, et al. Mitigating llm hallucinations via conformal abstention. *arXiv preprint arXiv:2405.01563*, 2024.
- Nick Yeung and Christopher Summerfield. Metacognition in human decision-making: confidence and error monitoring. *Philosophical Transactions of the Royal Society B: Biological Sciences*, 367(1594):1310–1321, 2012.
- Hanning Zhang, Shizhe Diao, Yong Lin, Yi Fung, Qing Lian, Xingyao Wang, Yangyi Chen, Heng Ji, and Tong Zhang. R-tuning: Instructing large language models to say ‘i don’t know’. In *Proceedings of*

the 2024 Conference of the North American Chapter of the Association for Computational Linguistics: Human Language Technologies (Volume 1: Long Papers), pages 7106–7132, 2024.

Author Contributions

DK conceived the project and experimental design. DK carried out the experiments and analysis with input from ND. VP, ND, PV, SO advised on the project. DK wrote the paper, with input from ND, VP, PV, and SO.

Acknowledgments

We thank Lewis Smith for advice, Charles Blundell for useful discussions, and Kim Stachenfeld for comments on an earlier version of the manuscript. We used Gemini to help improve the clarity and readability of part of the manuscript after the initial draft was completed.

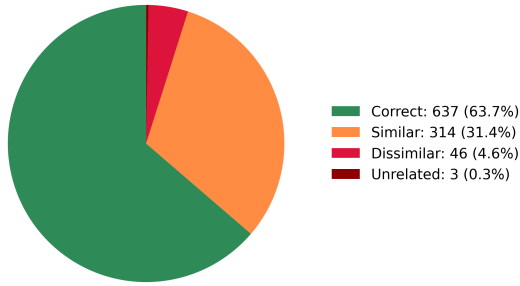
6 Supplemental Information

6.1 Supplemental Methods

Retrieval-Augmented Generation (RAG) Scores To quantify the accessibility of external knowledge relevant to each question, we computed retrieval-augmented generation (RAG) scores measuring the semantic overlap between questions and retrieved knowledge sources (Lewis et al., 2020). For each of the 1,000 questions, we queried the Wikipedia API (top 5 search results) and retrieved the first 500 characters of summary text from up to three accessible articles. Questions and retrieved contexts were embedded using the all-MiniLM-L6-v2 sentence transformer (Reimers and Gurevych, 2019), which produces 384-dimensional dense vector representations optimized for semantic similarity tasks. Cosine similarity was computed between each question embedding and its retrieved context embeddings. The RAG score for each question was defined as the maximum similarity across retrieved documents, representing the degree to which highly relevant external knowledge exists and can be successfully retrieved. Higher RAG scores indicate questions for which pertinent information is readily available in the knowledge corpus (Lewis et al., 2020). This measure is conceptually distinct from difficulty (aggregate model accuracy across prompts), confidence (internal metacognitive state), and semantic embeddings (structural question features), allowing us to test whether abstention behavior reflects knowledge accessibility versus other question characteristics. Retrieval succeeded for 680 of 1,000 questions (68%); failed retrievals received a RAG score of 0, indicating no accessible knowledge. Summary statistics: $M = 0.280$, $SD = 0.247$, median = 0.275, range = -0.165 to 0.918.

Question Semantic Embeddings To control for learned semantic and structural patterns in questions that might predict abstention independently of metacognitive confidence, we generated dense vector representations of all 1,000 questions. Questions were encoded using the all-MiniLM-L6-v2 sentence transformer (Reimers and Gurevych, 2019), a distilled model trained on over 1 billion sentence pairs that produces 384-dimensional embeddings optimized for semantic similarity tasks. This approach captures distributional semantic features (e.g., topic, domain, question type) that language models might use to implement learned heuristics for abstention (Bommasani et al., 2021). To reduce dimensionality and mitigate multicollinearity in regression models, we applied principal component analysis (PCA) to the 384-dimensional embeddings. We retained the first 10 principal components, which captured 23% of the variance while achieving a 97% reduction in dimensionality. This approach balances parsimony with representation of the primary axes of semantic variation across questions (Jolliffe and Cadima, 2016). Although 23% may appear modest, it reflects the distributed nature of modern sentence embeddings, where semantic information is encoded across the full high-dimensional space rather than concentrated in a few dominant dimensions (Ethayarajh, 2019). The retained components capture interpretable features such as topic domain, syntactic complexity, and question structure, while remaining orthogonal for regression analysis. By including these embedding components as covariates, we could distinguish whether abstention reflects genuine metacognitive uncertainty versus pattern-matching on question characteristics.

Phase 1: Standard 4-way MCQ
(No Abstention Option)



Phase 2: 4-way MCQ + Free Abstention Option

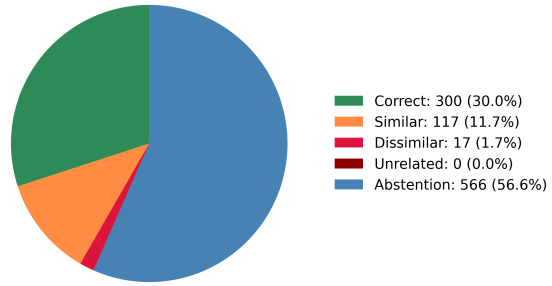


Figure 7: GPT4o: Performance on Phases 1 and 2. When the model makes errors it tends to pick similar foils, dissimilar and unrelated foils in decreasing order

Table 1: GPT-4o: Logistic regression predicting abstention in Phase 2

Predictor	Model A: Confidence Only			Model B: Full Model		
	Coef.	SE	z	Coef.	SE	z
Intercept	2.746***	0.262	10.49	3.923***	0.324	12.10
Confidence	-4.871***	0.470	-10.37	-5.263***	0.498	-10.56
Difficulty	-	-	-	0.342	0.265	1.29
RAG Score	-	-	-	-0.412	0.305	-1.35
Embedding PC6	-	-	-	0.106***	0.026	4.04
Embedding PC2	-	-	-	0.054**	0.021	2.59
Embedding PC4	-	-	-	-0.055*	0.022	-2.45
AIC	1227.4			1206.4		
Pseudo- R^2	0.106			0.139		

Notes. *** $p < 0.001$, **

$p < 0.01$, * $p < 0.05$. Difficulty = mean accuracy across seeds (higher = easier). Confidence = Phase 1 chosen confidence (0–1 scale). RAG Score = knowledge retrieval accessibility (0–1 scale). Embedding PCs = top 3 (by $|z|$) of 10 principal components from sentence embeddings; remaining 7 PCs included but not shown ($|z| < 1.5$). Model B provides a significantly better fit than Model A (LR $\chi^2(14) = 42.0$, $p = 1.4 \times 10^{-4}$, $\Delta AIC = -21.0$, $\Delta Pseudo-R^2 = 0.033$). Confidence remains the dominant predictor in standardized units ($|\beta_{std}| = 0.989$, $9.7\times$ larger than next-largest predictor).

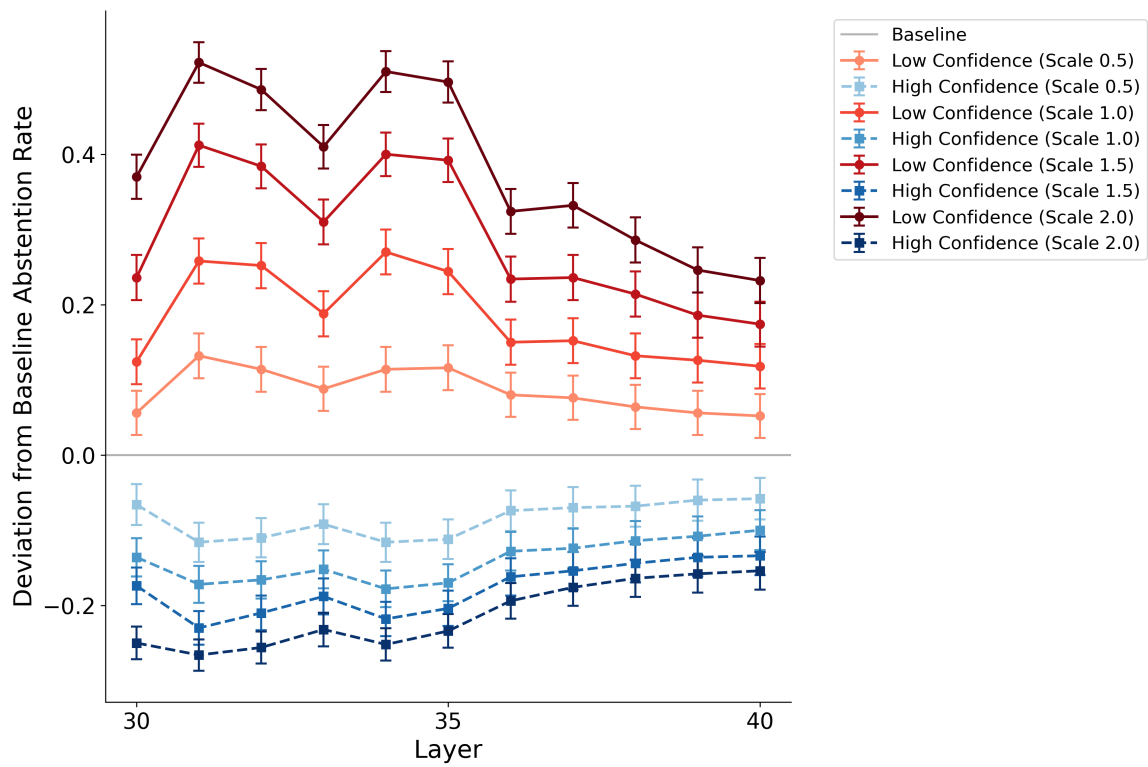


Figure 8: Gemma 3 27B: Change from baseline rate of abstention as a result of high and low confidence steering - focus on layers 30 to 40. Baseline level of abstention in no steering condition is 28.8%.

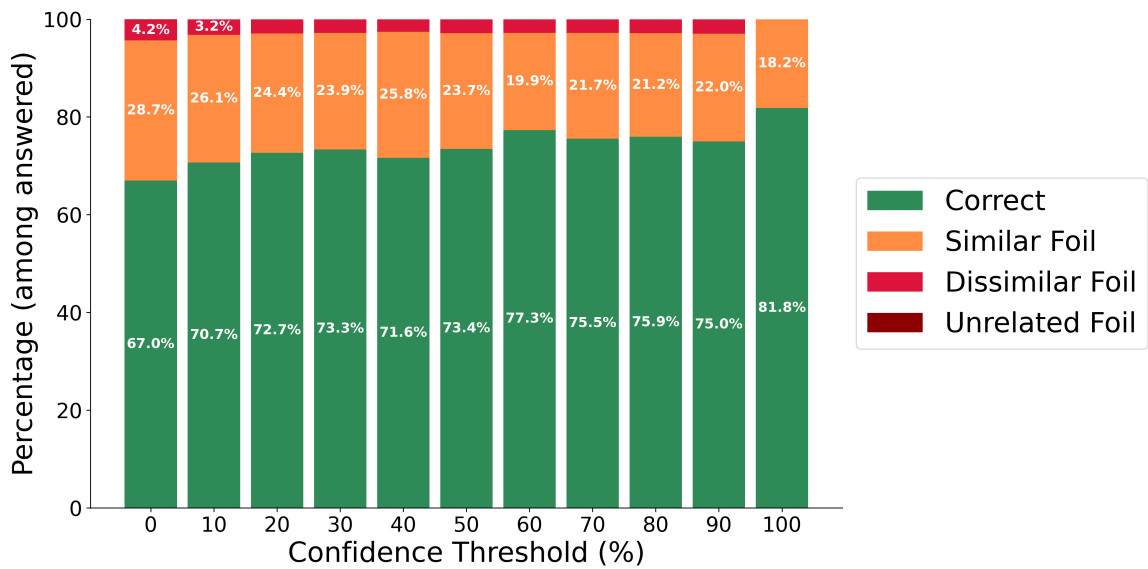


Figure 9: GPT4o Phase 4: Response breakdown among answered questions. Increasing threshold increases proportion of correct responses, whilst reducing frequency of similar and dissimilar errors.

6.2 Gemma Activation Steering: Mediation Analysis controlling for difficulty with Gemma specific covariate

We repeated the analysis including an explicit Gemma-specific difficulty covariate derived from the model’s own multiseed performance distribution (i.e., proportion correct over 20 runs, as conducted for GPT4o; $\mu = 0.565$, $\sigma = 0.291$, where 0 = hard and 1 = easy; correlation with GPT4o difficulty score $r = 0.44$, $p < 0.001$). When controlling for difficulty, the mediation pattern remained robust. Activation steering increased net confidence shift toward real options ($a = 0.107$, 95% CI [0.105, 0.110]), which in turn strongly reduced abstention odds ($b = -5.47$, 95% CI [-6.21, -4.76]), yielding an indirect effect of $a \times b = -0.59$ (95% CI [-0.67, -0.51]). The total effect of steering on abstention was $c = -0.83$, with a remaining direct effect of $c' = -0.30$ after accounting for the mediator. Item difficulty independently predicted lower abstention ($\gamma = -0.88$, $p < 0.001$), but the confidence-redistribution pathway still accounted for 70.5% of the total effect. Thus, even after controlling for Gemma’s own notion of difficulty, the mediation remained strong and significant, confirming that the confidence-based mechanism reflects a genuine causal driver rather than an artifact of differential item hardness.

6.3 GPT4o: Phase 4 confidence signals are postdecisional

To determine whether Phase 4 confidence signals are post-decisional—that is, whether they reflect the output of the abstention policy rather than the upstream beliefs that guide it—we examined how abstention rate varies as a joint function of instructed threshold and model confidence, comparing Phase 1 confidence (measured before abstention was possible) against Phase 4 confidence (measured after threshold instructions were given). If Phase 1 confidence represents a pre-decisional signal that is independently compared against the threshold, we would expect abstention to show a smooth diagonal gradient: increasing both as confidence decreases and as the threshold becomes stricter. In contrast, if Phase 4 confidence already incorporates the threshold instruction, we would expect abstention to collapse into horizontal bands determined almost entirely by the threshold-conditioned confidence, with threshold itself having little independent effect.

Figure 6 confirms this predicted dissociation. When abstention is plotted against Phase 1 confidence (Figure 6B), the heatmap exhibits the expected diagonal structure, indicating that threshold and confidence act as approximately independent inputs to a decision rule of the form $P(\text{abstain}) \approx \sigma((T - C)/\tau)$. By contrast, when abstention is plotted against Phase 4 confidence (Figure 6C), the heatmap collapses into largely horizontal bands: abstention varies almost entirely with confidence, and threshold has little independent effect. Quantitatively, the “bandness” index—computed as $(|r_C| - |r_T|)/(|r_C| + |r_T|)$ from the correlations of abstention with confidence (r_C) and threshold (r_T)—was near zero for Phase 1 confidence ($r_T = 0.63$, $r_C = -0.69$, index = 0.042) but strongly positive for Phase 4 confidence ($r_T = 0.11$, $r_C = -0.91$, index = 0.78) – with the low r_T indicating minor influence of threshold on abstention rate. This pattern indicates that Phase 4 confidence has already “baked in” the threshold instruction and reflects the output of the abstention policy rather than the upstream belief that originally guided the decision, providing direct evidence that Phase 4 confidence signals are post-decisional.

6.4 Phase 4: Logistic Regression Analysis of Abstention Confidence Data, GPT4o

Whilst our primary aim was to characterize the relationship between instructed thresholds, Phase 1 confidence and abstention behavior, for completeness we also analyzed the relationship between these predictors

Table 2: Phase 4: Logistic regression model predicting abstention, GPT4o.

Predictor	Coefficient (β)	Std. Error	z	p	
Intercept	3.417	0.109	31.43	< .001	
Threshold (T)	0.0327	0.00085	38.44	< .001	
Confidence (%)	-0.0582	0.00171	-34.11	< .001	
Difficulty	0.159	0.088	1.81	.071	<i>Notes.</i> Full model includes threshold,
RAG Score	-0.875	0.103	-8.47	< .001	
Embedding PC10	-0.043	0.010	-4.47	< .001	
Embedding PC3	-0.030	0.007	-4.11	< .001	
Embedding PC7	-0.036	0.009	-4.08	< .001	

confidence, difficulty, RAG score, and 10 embedding principal components (top 3 by $|z|$ shown; remaining 7 PCs: $|z| < 3.3$). Standardized effect sizes: Confidence ($|\beta_{\text{std}}| = 1.09$) and Threshold ($|\beta_{\text{std}}| = 1.03$) are comparable and substantially larger than RAG ($|\beta_{\text{std}}| = 0.22$), Difficulty ($|\beta_{\text{std}}| = 0.05$), and top embedding component ($|\beta_{\text{std}}| = 0.11$).

Table 3: Phase 4: Model comparison for abstention predictions, GPT4o.

Model	AIC (\downarrow)	pseudo- R^2 (\uparrow)	Key Likelihood Ratio Tests
Threshold only (T)	12874.3	0.105	–
T + Difficulty	12360.7	0.141	–
T + RAG	12765.8	0.113	–
T + Embeddings (10 PCs)	12778.1	0.114	–
T + Confidence	10921.0	0.241	vs. T: $\chi^2(1) = 1955.3, p < .001$ vs. T+RAG: $\chi^2(1) = 1897.9, p < .001$ vs. T+Embed: $\chi^2(1) = 1907.6, p < .001$
T + Confidence + Difficulty	10917.9	0.242	vs. T+Conf: $\chi^2(1) = 5.0, p = .025$
Full (all predictors)	10800.4	0.251	vs. T+Conf: $\chi^2(14) = 142.6, p < .001$

Notes. Full model includes threshold, confidence, difficulty, RAG score, and 10 embedding PCs. Confidence dominates all alternative predictors: adding confidence to models with T+RAG or T+Embeddings yields $\Delta\text{AIC} > 1800$, while adding RAG or embeddings to T+Confidence yields $\Delta\text{AIC} < 50$.

and the underlying driver of abstention behavior: a continuous variable, Phase 4 confidence in the abstention choice (see Figure 10).

To do this, we performed a linear regression with a nested model that was directly analogous to that used to analyze binary abstention data. The analysis of phase 3 abstention confidence similarly revealed systematic effects of both instructed threshold and phase 1 chosen confidence. Abstention confidence increased with higher instructed thresholds ($\beta_T = 0.0033$, SE= 0.000050, $z = 65.6$, $p < 0.001$), and decreased sharply as phase 1 chosen confidence increased ($\beta_C = -0.0042$, SE= 0.00011, $z = -39.5$, $p < 0.001$). In practical terms, this means that raising the instructed threshold by 20 points increased the model’s abstention confidence by 0.066 (on the 0–1 scale). A 20-point increase in chosen confidence reduced abstention confidence by 0.084. Therefore, the more confident the model was in its initial choice – and the lower the instructed threshold – the less probability mass it assigned to the abstention option. Item difficulty had a statistically significant but small effect ($\beta_D = 0.038$, SE= 0.0060, $z = 6.39$, $p < 0.001$), though its magnitude was minor compared to threshold and confidence: from the hardest to easiest items, abstention confidence increased by only 3.8 percentage points. The full model explained 36.1% of variance ($R^2 = 0.361$). Confidence was the dominant predictor, improving model fit five times more than difficulty when

added to the baseline threshold model (confidence: $\Delta R^2 = 0.109$, $\Delta AIC = -1731$; difficulty: $\Delta R^2 = 0.021$, $\Delta AIC = -312$).

These findings parallel the results of the binary abstention analyses: both demonstrate that abstention behavior is jointly shaped by instructed threshold and the model’s own pre-decisional (i.e. phase 1) confidence. Together, our analyses of abstention confidence demonstrate that instructed threshold shifts the model toward abstention even before the decision boundary is crossed, while confidence pulls it back toward answering — providing convergent evidence, via a richer signal, for the same underlying mechanism identified in the binary analyses.

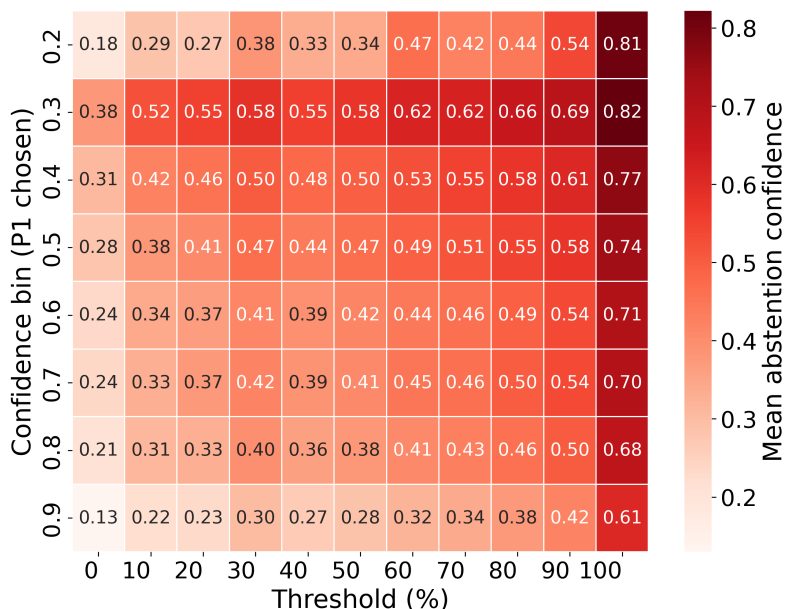


Figure 10: Heatmap of GPT-4o’s abstention confidence in Phase 4, shown as a function of instructed threshold and Phase 1 chosen confidence. Warmer colors indicate stronger abstention confidence, also specified by numbers inside cells. The continuous abstention confidence reveals a linear additive structure: abstention confidence increases steadily with instructed threshold and decreases steadily with chosen confidence, with difficulty having only a minor influence. See Main text for details

6.5 Gemma 3 27B Results

6.5.1 Phase 1 and 2 Results for Gemma 3 27B

Gemma 3 performed at 55.1% correct during phase 1 where there was a 4-way choice between available answers, with no option to abstain. We calibrated the model using the temperature scaling method of (Guo et al., 2017)(see Methods), resulting in an optimal scaling temperature of 5.1 (ECE = 0.049; AUROC = 0.81). There was a robust relationship between calibrated confidence and error rate on the Phase 1 test dataset, with higher confidence strongly predicting correct responses (Figure 11).

In phase 2, the model was exposed to the same multiple choice questions, but had the additional option to abstain. Here performance was 41.6% correct, 31.2% incorrect, and 27.2% abstention. Accuracy on answered questions was higher in phase 2 compared to phase 1 (60.5% vs 55.1%), with coverage reduced from 100% to 68.8%.

A logistic regression analysis (see Methods) revealed that question difficulty alone (see difficulty score in

Methods) provided a degree of predictive power (AIC = 1143.8, pseudo- R^2 = 0.026, β_D = -1.22, SE = 0.22, z = -5.49, p < 0.001). Because Gemma and GPT4o were evaluated on the same multiple-choice items, we used the multi-seed GPT4o difficulty score as an external measure of item hardness. This score reflects the expected probability of a correct answer across random answer-choice allocations, providing a model-agnostic estimate of how objectively hard each question is.

Importantly, adding the model’s chosen confidence from Phase 1 improved model fit (AIC = 1077.9, change in AIC = -65.9, pseudo- R^2 = 0.084, LR $\chi^2(1)$ = 67.85, p < 0.001). In the full model, difficulty remained significant (β_D = -0.84, SE = 0.24, z = -3.55, p < 0.001). The confidence effect was prominent (β_C = -5.57, SE = 0.70, z = -7.94, p < 0.001), indicating that higher confidence strongly reduces abstention probability (see Table 4). In practical terms, a 0.1-unit increase in confidence (e.g., from 0.7 to 0.8) reduces the abstention odds by approximately 43% (odds ratio = 0.57).

Whilst an explicit threshold for abstention was not stated in the instructions to the model in Phase 2, the form of our logistic regression model allows us to infer a fitted threshold that underlies the model’s behavior (see Methods). We found the confidence level at which the model abstains 50% of the time, the indifference point T_{50} , to be approximately 38.4% (holding difficulty constant at the sample mean of 0.66) – with the policy temperature parameter of 0.18 units (equivalent to $1/|\beta_C|$) (see Figure 11B).

Table 4: Gemma 27B: Logistic regression predicting abstention in Phase 2

Predictor	Model A: Difficulty Only			Model B: Difficulty + Confidence			
	Coef.	SE	z	Coef.	SE	z	
Intercept	-0.234	0.149	-1.56	2.692***	0.399	6.75	
Difficulty	-1.215***	0.221	-5.49	-0.837***	0.236	-3.55	<i>Notes.</i> *** p < 0.001. Difficulty
Confidence	-	-	-	-5.575***	0.702	-7.94	
AIC		1143.8			1077.9		
Pseudo- R^2		0.026			0.084		

= mean accuracy across seeds (higher = easier). Confidence = Phase 1 chosen confidence.

6.5.2 Gemma 3 27B, Phase 4: Analysis of Performance

The prompt used for GPT-4o proved ineffective for Gemma 3 27b, yielding abstention rates of below 5% until the 80% threshold and only averaging 34.4% above this threshold. This resulted in insufficient variance and no significant threshold effect in the logistic regression (β = 0.0012 \pm 0.001, z = 1.71, p = 0.086).

To establish robust abstention behavior, we generated 20 paraphrases of the basic GPT4o prompt using Gemini 2.5 Pro while preserving meaning and answer format. As shown in Figure 12, this strategy was successful: 13 of the 20 prompts exceeded 80% abstention at the 100% threshold, confirming that appropriate prompt framing is critical for eliciting reliable abstention behavior in this model. We used the prompt with the highest (i.e. 100%) abstention rate at the 100% instructed threshold for the main experiment (see Methods for prompt used).

We first examined the overall pattern of correct, incorrect and abstention responses showed by the model. As expected, there was a clear effect of threshold on abstention rate – with increasing abstention rates as the threshold was increased (see Figure 11C).

We first examined whether abstention behavior was systematically shaped by the instructed threshold, and whether this influence was modulated by the model’s own confidence (Figure 11D). As for GPT4o, for

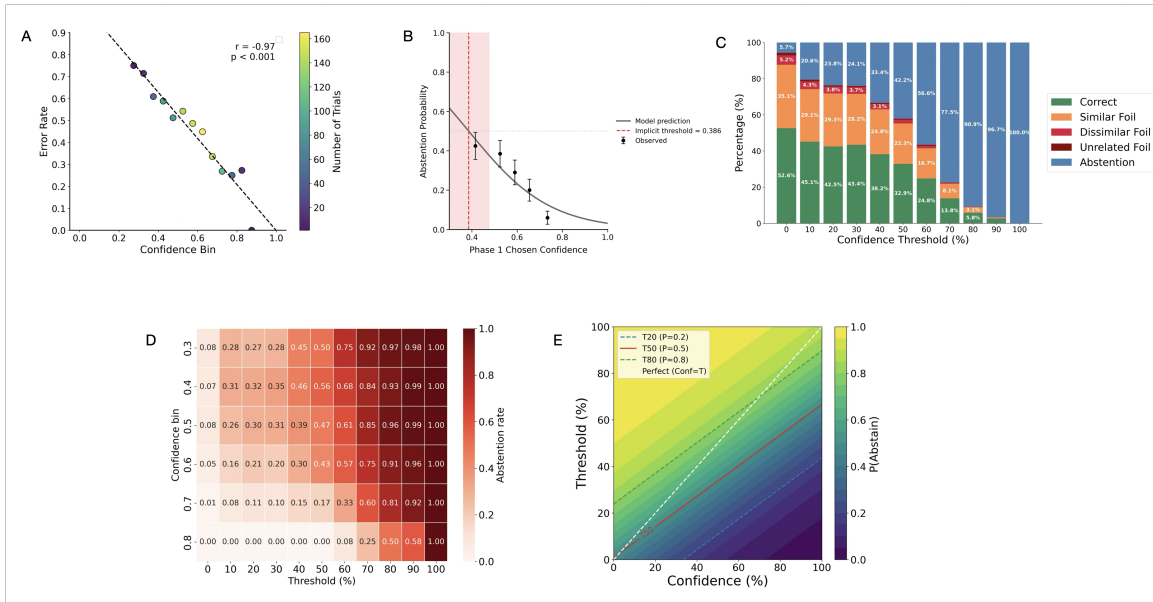


Figure 11: **Gemma 3 27B results across phases 1,2 and 4.**(A) Gemma 27B confidence predicts error rate (Phase 1).Relationship between binned confidence and error rate in Phase 1. Each point represents a confidence bin (width = 0.05); color encodes the number of trials. A strong negative correlation was observed between confidence and error rate ($r = -0.97$, $p < 0.001$). Model was calibrated on a separate set of 1000 trials (see Methods). (B) Gemma 27B confidence predicts abstention behavior (phase 2). Logistic regression model of natural abstention probability as a function of confidence for $n = 1000$ trials. The grey curve indicates the model prediction, fitted to individual binary abstention decisions. The red dashed line marks the implicit decision threshold at 38.6%, where $P(\text{abstain}) = 0.5$ (holding difficulty constant at sample mean). The red shaded region denotes the confidence interval spanning approximately ± 9 percentage points around the threshold, illustrating the sharpness/softness of the decision boundary (policy temperature = 0.18 units, or 18 percentage points). Black circles represent observed abstention rates (mean \pm 95% CI) across confidence quintiles. The low threshold (38.6%) indicates that Gemma 27B continues answering even at relatively low confidence levels, only choosing to abstain when confidence drops below this point, revealing the model’s intrinsic abstention boundary even without explicit threshold instructions. (C) Performance of Gemma 27B in Phase 4 as a function of instructed threshold. (D) Profile of abstention behavior shown by Gemma in phase 4, as a function of Phase 1 confidence and instructed threshold. Abstention rate (0-1) increases from left to right (instructed threshold), and from bottom to top (binned confidence). Confidence: calibrated chosen confidence from phase 1, binned into fixed bins of size 0.1 (in the range 0.3-1.0). (E) Decision rule guiding abstention behavior shown by fitted model. Behavior of perfectly calibrated model shown along the diagonal (i.e. Conf = Threshold). In comparison, the fitted model is moderately conservative due to under-weighting its own confidence relative to the instructed threshold (scale = 0.66), such that a 1% increase in confidence offsets only approximately 0.66% of threshold. The baseline bias (shift = +1.0%) is negligible. Contours T_{20} , T_{50} , T_{80} mark thresholds at which the model abstains with 20%, 50%, 80% probability. Points to the right/below each line correspond to lower abstention rates, while points to the left/above correspond to higher abstention rates. The moderate gap between T_{20} and T_{80} reflects a moderately soft transition (policy temperature = 16.6) of the decision boundary.

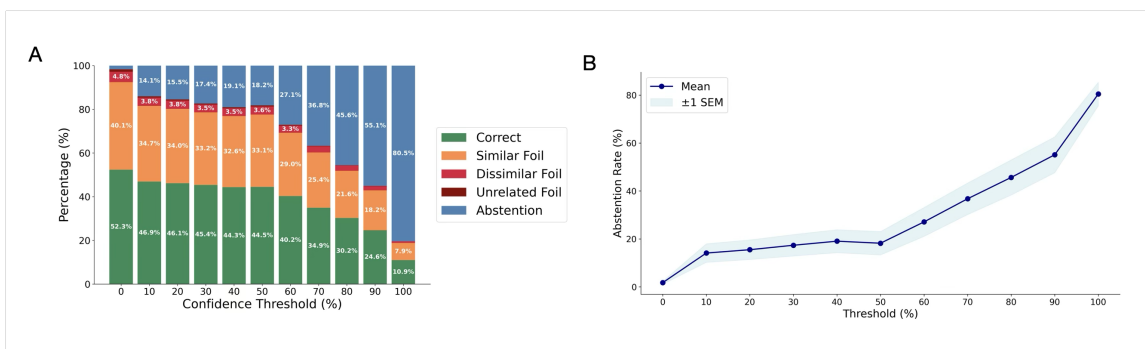


Figure 12: **Performance of Gemma 27B on Phase 4 averaged across 20 prompts.** (A) Performance of Gemma 3 27B averaged across 20 prompts (see Methods for details). (B) Abstention rate as a function of instructed threshold, averaged across 20 prompts.

this analysis we used chosen confidence estimates from phase 1, since these were elicited in the absence of an abstention option.

6.5.3 Gemma 27B: Computational Modeling of binary abstention data, Phase 4

We next sought to fit a quantitative model to the profile of abstention behavior observed. Specifically, we asked whether chosen confidence from phase 1 was a robust predictor of abstention behavior, above and beyond any effects of instructed threshold and difficulty. To do this, we set up a nested logistic regression model whose dependent variable was binary abstention decisions, and included predictors for chosen confidence, instructed threshold, and our measure of question difficulty. We found that a model that included chosen confidence, threshold and difficulty predictors (AIC = 9544.4; pseudo- $R^2 = 0.374$) outperformed baseline models that included either threshold only (AIC = 10021.8; pseudo- $R^2 = 0.342$) or threshold and difficulty (AIC = 9824.5; pseudo- $R^2 = 0.355$) or threshold and confidence (AIC = 9632.0; pseudo- $R^2 = 0.368$) (see Table 6). As such, a likelihood ratio test (LRT) showed a highly significant benefit for the addition of confidence to a threshold and difficulty model ($\chi^2(1) = 282.15$, $p < 0.001$). These results, therefore, provide robust evidence that both instructed threshold and phase 1 chosen confidence markedly influence abstention behavior.

We next examined the fitted coefficients. This indicated that abstention rate increased with threshold ($\beta_T = 0.060$, SE= 0.0011, $z = 55.4$, $p < 0.001$) and decreased with confidence ($\beta_C = -0.040$, SE= 0.0024, $z = -16.4$, $p < 0.001$). Difficulty was also significant ($\beta_D = -0.78$, SE= 0.083, $z = -9.40$, $p < 0.001$), consistent with a greater tendency to abstain on harder items (see Table 5). We derived three interpretable quantities: scale (sensitivity to confidence relative to threshold; 0.66), shift (baseline abstention bias; +1.0), and policy temperature (softness of the boundary; 16.6). We also computed the indifference threshold, T_{50} , at which the model is equally likely to answer or abstain: for example, at a confidence level of 80% the model’s indifference point is a threshold of approximately 53.5% (see Figure 11E). Given that a perfectly calibrated model abstains when its own confidence is equal to the instructed threshold (assuming symmetric costs), this result indicates that the model is moderately conservative in its tendency to abstain. The scale parameter of 0.66 indicates that the model under-weights its own confidence relative to the instructed threshold: a 1% increase in confidence offsets only approximately 0.66% of threshold.

Table 5: Gemma 3 27B: Logistic regression predicting abstention (Phase 4), Full model

Predictor	Coefficient (β)	Std. Error	z	p
Intercept	-0.058	0.138	-0.42	.673
Threshold (T)	0.060	0.0011	55.35	< .001
Confidence (%)	-0.040	0.0024	-16.42	< .001
Difficulty	-0.778	0.083	-9.40	< .001

Table 6: Gemma 3 27B: Model comparison for abstention predictions (Phase 4)

Model	AIC (\downarrow)	pseudo- R^2 (\uparrow)	Key Likelihood Ratio Tests
Threshold only (T)	10021.8	0.342	–
Threshold + Confidence	9632.0	0.368	vs. T: $\chi^2(1) = 391.82, p < .001$
Threshold + Difficulty	9824.5	0.355	–
Full (T + Confidence + Difficulty)	9544.4	0.374	vs. T+Conf: $\chi^2(1) = 89.62, p < .001$

6.6 Results for DeepSeek 671B

6.6.1 Phase 1 and 2 Results for DeepSeek 671B

DeepSeek 671B performed at 67.7% correct during phase 1 where there was a 4-way choice between available answers, with no option to abstain. We calibrated the model using the temperature scaling method of (Guo et al., 2017)(see Methods), resulting in an optimal scaling temperature of 29.3 (ECE = 0.0065; AUROC = 0.83). A high scaling temperature was required since the model was very overconfident pre-calibration. There was a robust relationship between calibrated confidence and error rate on the Phase 1 test dataset, with higher confidence strongly predicting correct responses (Figure 13).

In phase 2, the model was exposed to the same multiple choice questions, but had the additional option to abstain. Here performance was 13.8% correct, 4.2% incorrect, and 82.0% abstention. Accuracy on answered questions was higher in phase 2 compared to phase 1 (76.7% vs 67.7%), with coverage reduced from 100% to 83.0%.

A logistic regression analysis (see Methods) revealed that question difficulty alone (see difficulty score in Methods) provided a degree of predictive power (AIC = 930.9, pseudo- $R^2 = 0.017$, $\beta_D = -1.06$, SE = 0.27, $z = -3.88$, $p < 0.001$). Because DeepSeek and GPT4o were evaluated on the same multiple-choice items, we used the multi-seed GPT4o difficulty score as an external measure of item hardness. This score reflects the expected probability of a correct answer across random answer-choice allocations, providing a model-agnostic estimate of how objectively hard each question is.

Adding the model’s chosen confidence from Phase 1 substantially improved model fit (AIC = 817.7, change in AIC = -113.2, pseudo- $R^2 = 0.139$, LR $\chi^2(1) = 115.21$, $p < 0.001$). In the full model, difficulty became non-significant ($\beta_D = -0.48$, SE = 0.29, $z = -1.66$, $p = 0.097$). The confidence effect was highly prominent ($\beta_C = -5.46$, SE = 0.53, $z = -10.28$, $p < 0.001$), indicating that higher confidence strongly reduces abstention probability (see Table 7). In practical terms, a 0.1-unit increase in confidence (e.g., from 0.7 to 0.8) reduces the abstention odds by approximately 42% (odds ratio = 0.58).

Whilst an explicit threshold for abstention was not stated in the instructions to the model in Phase 2, the form of our logistic regression model allows us to infer a fitted threshold that underlies the model’s behavior (see Methods). We found the confidence level at which the model abstains 50% of the time, the

indifference point T_{50} , to be approximately 74.2% (holding difficulty constant at the sample mean of 0.65) – with the policy temperature parameter of 0.18 units (equivalent to $1/|\beta_C|$) (see Figure 13B).

Table 7: DeepSeek 671B: Logistic regression predicting abstention in Phase 2

Predictor	Model A: Difficulty Only			Model B: Difficulty + Confidence			
	Coef.	SE	z	Coef.	SE	z	
Intercept	2.238***	0.212	10.55	4.364***	0.313	13.96	<i>Notes.</i> *** $p < 0.001$. Difficulty
Difficulty	-1.060***	0.273	-3.88	-0.481	0.290	-1.66	
Confidence	-	-	-	-5.461***	0.531	-10.28	
AIC		930.9			817.7		
Pseudo- R^2		0.017			0.139		

= mean accuracy across seeds (higher = easier). Confidence = Phase 1 chosen confidence.

6.6.2 DeepSeek 671B, Phase 4: Analysis of Performance

We first examined the overall pattern of correct, incorrect and abstention responses showed by the model. As expected, there was a clear effect of threshold on abstention rate – with increasing abstention rates as the threshold was increased (see Figure 13C).

We first examined whether abstention behavior was systematically shaped by the instructed threshold, and whether this influence was modulated by the model’s own confidence (Figure 13D). As before, we used chosen confidence estimates from phase 1, since these were elicited in the absence of an abstention option.

6.6.3 DeepSeek 671B: Computational Modeling of binary abstention data, Phase 4

We next sought to fit a quantitative model to the profile of abstention behavior observed. Specifically, we asked whether chosen confidence from phase 1 was a robust predictor of abstention behavior, above and beyond any effects of instructed threshold and difficulty. To do this, we set up a nested logistic regression model whose dependent variable was binary abstention decisions, and included predictors for chosen confidence, instructed threshold, and our measure of question difficulty. We found that a model that included chosen confidence, threshold and difficulty predictors (AIC = 13206.1; pseudo- R^2 = 0.132) outperformed baseline models that included either threshold only (AIC = 13798.3; pseudo- R^2 = 0.092) or threshold and difficulty (AIC = 13540.5; pseudo- R^2 = 0.109) or threshold and confidence (AIC = 13354.3; pseudo- R^2 = 0.122) (see Table 9). As such, a likelihood ratio test (LRT) showed a highly significant benefit for the addition of confidence to a threshold and difficulty model ($\chi^2(1) = 336.46$, $p < 0.001$). These results, therefore, provide robust evidence that both instructed threshold and phase 1 chosen confidence markedly influence abstention behavior.

We next examined the fitted coefficients. This indicated that abstention rate increased with threshold ($\beta_T = 0.025$, SE= 0.00071, $z = 35.9$, $p < 0.001$) and decreased with confidence ($\beta_C = -0.027$, SE= 0.0015, $z = -17.6$, $p < 0.001$). Difficulty was also significant ($\beta_D = -0.81$, SE= 0.066, $z = -12.2$, $p < 0.001$), consistent with a greater tendency to abstain on harder items (see Table 8). We derived three interpretable quantities: scale (sensitivity to confidence relative to threshold; 1.05), shift (baseline abstention bias; -8.5), and policy temperature (softness of the boundary; 39.3). We also computed the indifference threshold, T_{50} , at which the model is equally likely to answer or abstain: for example, at a confidence level of 80% the model’s indifference point is a threshold of approximately 75.7% (see Figure 13E). Given that a perfectly

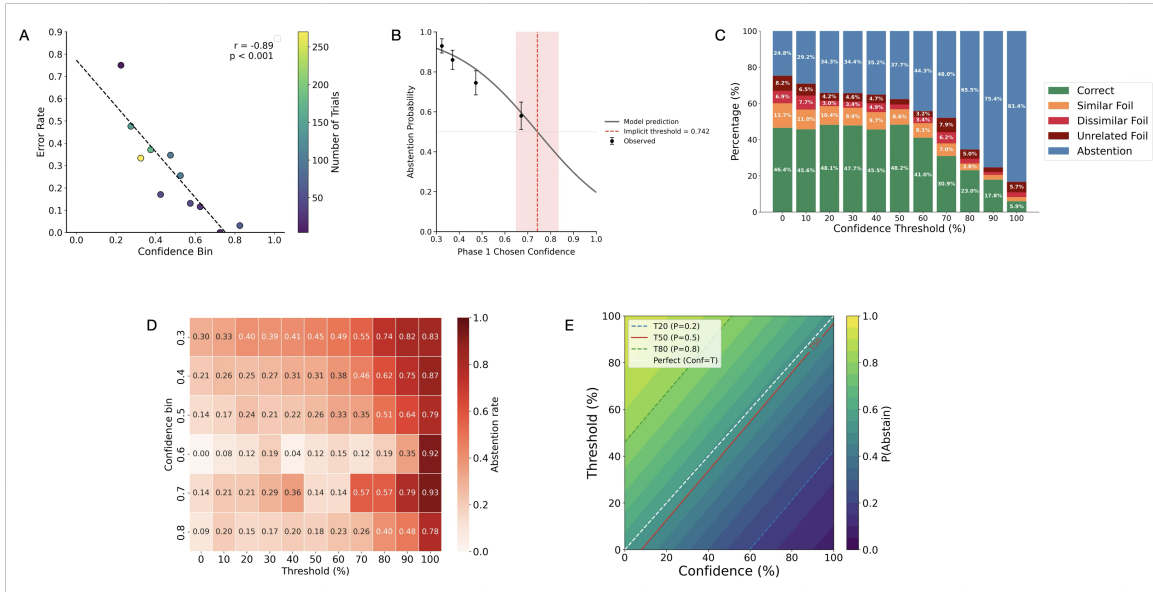


Figure 13: **DeepSeek 671B results across phases 1,2 and 4.**(A) DeepSeek 671B confidence predicts error rate (Phase 1). Relationship between binned confidence and error rate in Phase 1. Each point represents a confidence bin (width = 0.05); color encodes the number of trials. A strong negative correlation was observed between confidence and error rate. Model was calibrated on a separate set of 1000 trials (see Methods). (B) DeepSeek 671B confidence predicts abstinence behavior (phase 2). Logistic regression model of natural abstinence probability as a function of confidence for $n = 1000$ trials. The grey curve indicates the model prediction, fitted to individual binary abstinence decisions. The red dashed line marks the implicit decision threshold at 74.2%, where $P(\text{abstain}) = 0.5$ (holding difficulty constant at sample mean). The red shaded region denotes the confidence interval spanning approximately ± 9 percentage points around the threshold, illustrating the sharpness/softness of the decision boundary (policy temperature = 0.18 units, or 18 percentage points). Black circles represent observed abstinence rates (mean \pm 95% CI) across confidence quintiles. The high threshold (74.2%) indicates that DeepSeek requires relatively high confidence before choosing to answer, readily abstaining when confidence drops below this point, revealing the model’s intrinsic abstinence boundary even without explicit threshold instructions. (C) Performance of DeepSeek in Phase 4 as a function of instructed threshold. (D) Profile of abstinence behavior shown by DeepSeek in phase 4, as a function of confidence and instructed threshold. Confidence: calibrated chosen confidence from phase 1, binned into fixed bins of size 0.1 (in the range 0.3- 0.9). (E) Decision rule guiding abstinence behavior shown by fitted model. Behavior of perfectly calibrated model shown along the diagonal (i.e. Conf = Threshold). The fitted model exhibits near-perfect calibration with essentially equal weighting of confidence and threshold (scale = 1.05), such that a 1% increase in confidence offsets approximately 1.05% of threshold. The baseline bias is minimal (shift = -8.5%). Contours T_{20} , T_{50} , T_{80} mark thresholds at which the model abstains with 20%, 50%, 80% probability. Points to the right/below each line correspond to lower abstinence rates, while points to the left/above correspond to higher abstinence rates. The wide gap between T_{20} and T_{80} reflects a relatively soft transition (policy temperature = 39.3) of the decision boundary, indicating gradual rather than sharp changes in abstinence probability across the confidence-threshold space.

calibrated model abstains when its own confidence is equal to the instructed threshold, this result indicates that the model is essentially well-calibrated with near-equal weighting of confidence and threshold. The scale parameter of 1.05 indicates that the model appropriately weights its own confidence relative to the instructed threshold: a 1% increase in confidence offsets approximately 1.05% of threshold.

Table 8: DeepSeek 671B: Logistic regression predicting abstention (Phase 4), Full model

Predictor	Coefficient (β)	Std. Error	z	p
Intercept	0.216	0.077	2.81	.005
Threshold (T)	0.025	0.00071	35.93	< .001
Confidence (%)	-0.027	0.0015	-17.64	< .001
Difficulty	-0.810	0.066	-12.19	< .001

Table 9: DeepSeek 671B: Model comparison for abstention predictions (Phase 4)

Model	AIC (\downarrow)	pseudo- R^2 (\uparrow)	Key Likelihood Ratio Tests
Threshold only (T)	13798.3	0.092	–
Threshold + Confidence	13354.3	0.122	vs. T: $\chi^2(1) = 445.93, p < .001$
Threshold + Difficulty	13540.5	0.109	–
Full (T + Confidence + Difficulty)	13206.1	0.132	vs. T+Conf: $\chi^2(1) = 150.26, p < .001$

6.7 Results for Qwen 80B

6.7.1 Phase 1 and 2 Results for Qwen 80B

Qwen 80B performed at 65.8% correct during phase 1 where there was a 4-way choice between available answers, with no option to abstain. We calibrated the model using the temperature scaling method of (Guo et al., 2017)(see Methods), resulting in an optimal scaling temperature of 4.9 (ECE = 0.078; AUROC = 0.89). There was a robust relationship between calibrated confidence and error rate on the Phase 1 test dataset, with higher confidence strongly predicting correct responses (Figure 14).

In phase 2, the model was exposed to the same multiple choice questions, but had the additional option to abstain. Here performance was 40.1% correct, 16.1% incorrect, and 43.8% abstention. Accuracy on answered questions was higher in phase 2 compared to phase 1 (73.1% vs 65.8%), with coverage reduced from 100% to 56.2%.

A logistic regression analysis (see Methods) revealed that question difficulty alone (see difficulty score in Methods) provided a degree of predictive power (AIC = 1360.0, pseudo- $R^2 = 0.011$, $\beta_D = -0.76$, SE = 0.20, $z = -3.84$, $p < 0.001$). Because Qwen 80B and GPT4o were evaluated on the same multiple-choice items, we used the multi-seed GPT4o difficulty score as an external measure of item hardness. This score reflects the expected probability of a correct answer across random answer-choice allocations, providing a model-agnostic estimate of how objectively hard each question is.

Adding the model’s chosen confidence from Phase 1 substantially improved model fit (AIC = 1256.6, change in AIC = -103.3, pseudo- $R^2 = 0.088$, LR $\chi^2(1) = 105.34$, $p < 0.001$). In the full model, difficulty became non-significant ($\beta_D = 0.04$, SE = 0.23, $z = 0.18$, $p = 0.857$). The confidence effect was highly prominent ($\beta_C = -4.51$, SE = 0.46, $z = -9.73$, $p < 0.001$), indicating that higher confidence strongly

reduces abstention probability (see Table 10). In practical terms, a 0.1-unit increase in confidence (e.g., from 0.7 to 0.8) reduces the abstention odds by approximately 36% (odds ratio = 0.64).

Whilst an explicit threshold for abstention was not stated in the instructions to the model in Phase 2, the form of our logistic regression model allows us to infer a fitted threshold that underlies the model’s behavior (see Methods). We found the confidence level at which the model abstains 50% of the time, the indifference point T_{50} , to be approximately 67.5% (holding difficulty constant at the sample mean) – with the policy temperature parameter of 0.22 units (equivalent to $1/|\beta_C|$) (see Figure 14B).

Table 10: Qwen 80B: Logistic regression predicting abstention in Phase 2

Predictor	Model A: Difficulty Only			Model B: Difficulty + Confidence		
	Coef.	SE	z	Coef.	SE	z
Intercept	0.241	0.142	1.70	3.017***	0.323	9.34
Difficulty	-0.765***	0.199	-3.84	0.041	0.227	0.18
Confidence	-	-	-	-4.510***	0.463	-9.73
AIC	1360.0			1256.6		
Pseudo- R^2	0.011			0.088		

Notes. *** $p < 0.001$. Difficulty

= mean accuracy across seeds (higher = easier). Confidence = Phase 1 chosen confidence.

6.7.2 Qwen 80B, Phase 4: Analysis of Performance

We first examined the overall pattern of correct, incorrect and abstention responses showed by the model. As expected, there was a clear effect of threshold on abstention rate – with increasing abstention rates as the threshold was increased (see Figure 14C).

We first examined whether abstention behavior was systematically shaped by the instructed threshold, and whether this influence was modulated by the model’s own confidence (Figure 14D). As before, we used chosen confidence estimates from phase 1, since these were elicited in the absence of an abstention option.

6.7.3 Qwen 80B: Computational Modeling of binary abstention data, Phase 4

We next sought to fit a quantitative model to the profile of abstention behavior observed. Specifically, we asked whether chosen confidence from phase 1 was a robust predictor of abstention behavior, above and beyond any effects of instructed threshold and difficulty. To do this, we set up a nested logistic regression model whose dependent variable was binary abstention decisions, and included predictors for chosen confidence, instructed threshold, and our measure of question difficulty. We found that a model that included chosen confidence, threshold and difficulty predictors (AIC = 10961.1; pseudo- R^2 = 0.207) outperformed baseline models that included either threshold only (AIC = 12284.5; pseudo- R^2 = 0.111) or threshold and difficulty (AIC = 12062.4; pseudo- R^2 = 0.127). The contribution of difficulty in the full model was near zero: a model including only threshold and confidence had a comparable fit as the full model (AIC = 10962.7; pseudo- R^2 = 0.207) (see Table 12). As such, a likelihood ratio test (LRT) showed a highly significant benefit for the addition of confidence to a threshold and difficulty model ($\chi^2(1) = 1103.35$, $p < 0.001$). These results, therefore, provide robust evidence that both instructed threshold and phase 1 chosen confidence markedly influence abstention behavior.

We next examined the fitted coefficients. This indicated that abstention rate increased with threshold ($\beta_T = 0.034$, SE= 0.0009, $z = 37.9$, $p < 0.001$) and decreased with confidence ($\beta_C = -0.051$, SE= 0.0016,

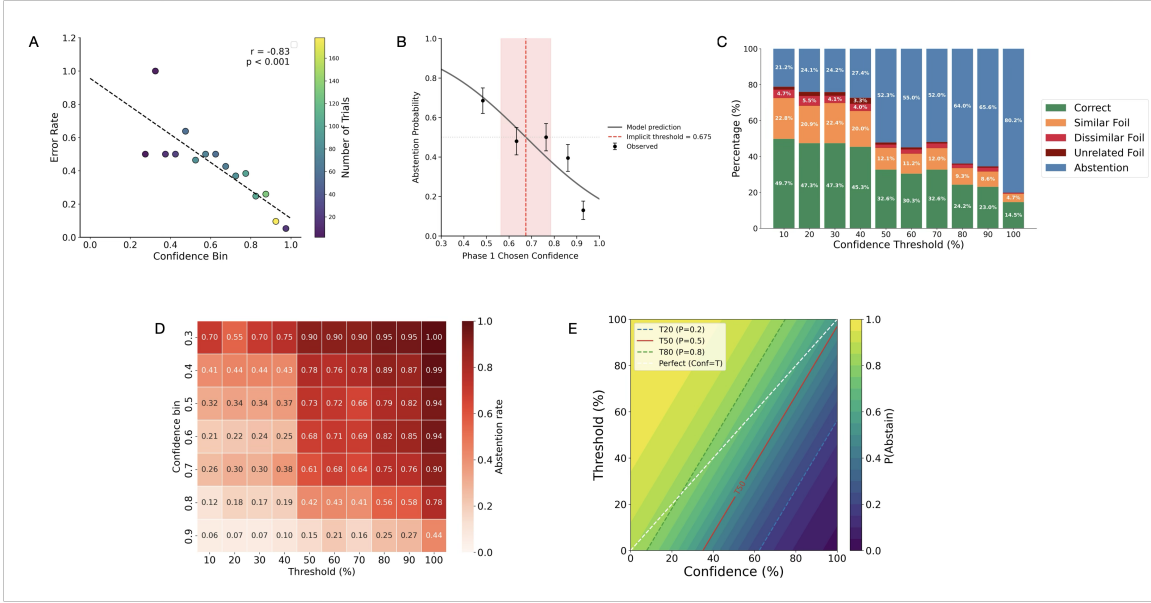


Figure 14: **Qwen 80B results across phases 1,2 and 4.**(A) Qwen 80B confidence predicts error rate (Phase 1). Relationship between binned confidence and error rate in Phase 1. Each point represents a confidence bin (width = 0.05); color encodes the number of trials. A strong negative correlation was observed between confidence and error rate. Model was calibrated on a separate set of 1000 trials (see Methods). (B) Qwen 80B confidence predicts abstention behavior (phase 2). Logistic regression model of natural abstention probability as a function of confidence for $n = 1000$ trials. The grey curve indicates the model prediction, fitted to individual binary abstention decisions. The red dashed line marks the implicit decision threshold at 67.5%, where $P(\text{abstain}) = 0.5$ (holding difficulty constant at sample mean of 0.646). The red shaded region denotes the confidence interval spanning approximately ± 11 percentage points around the threshold, illustrating the sharpness/softness of the decision boundary (policy temperature = 0.22 units, or 22 percentage points). Black circles represent observed abstention rates (mean \pm 95% CI) across confidence quintiles. The moderately high threshold (67.5%) indicates that Qwen 80B requires relatively high confidence before choosing to answer, readily abstaining when confidence drops below this point, revealing the model’s intrinsic abstention boundary even without explicit threshold instructions.(C) Performance of Qwen 80B in Phase 4 as a function of instructed threshold. (D) Profile of abstention behavior shown by Qwen 80B in phase 4, as a function of confidence and instructed threshold. Confidence: calibrated chosen confidence from phase 1, binned into fixed bins of size 0.1 (in the range 0.3- 1.0). (E) Decision rule guiding abstention behavior shown by fitted model. Behavior of perfectly calibrated model shown along the diagonal (i.e. Conf = Threshold). The fitted model substantially over-weights internal confidence relative to instructed threshold (scale = 1.49), such that a 1% increase in confidence offsets approximately 1.49% of threshold. The large negative shift (-52.3%) means that at very low confidence levels the model is overly cautious, but the high scale parameter causes the decision boundary to tilt steeply, such that at higher confidence levels (above 50%) the model becomes increasingly over-confident and answers more readily than a perfectly calibrated model would. Contours T_{20} , T_{50} , T_{80} mark thresholds at which the model abstains with 20%, 50%, 80% probability. Points to the right/below each line correspond to lower abstention rates, while points to the left/above correspond to higher abstention rates. The relatively wide gap between T_{20} and T_{80} reflects a moderately soft transition (policy temperature = 29.3 in percent units) of the decision boundary.

$z = -31.0$, $p < 0.001$). Difficulty was marginally non-significant ($\beta_D = -0.148$, SE= 0.077, $z = -1.91$, $p = 0.056$) (see Table 11). We derived three interpretable quantities: scale (sensitivity to confidence relative to threshold; 1.49), shift (baseline abstention bias; -52.3), and policy temperature (softness of the boundary; 29.3 in percent units, or 0.29 in 0–1 units). We also computed the indifference threshold, T_{50} , at which the model is equally likely to answer or abstain: for example, at a confidence level of 80% the model’s indifference point is a threshold of approximately 67.1% (see Figure 14E). The scale parameter of 1.49 indicates that the model weights its own confidence considerably more heavily than the instructed threshold: a 1% increase in confidence offsets approximately 1.49% of threshold. Given that a perfectly calibrated model abstains when its own confidence is equal to the instructed threshold, this result indicates that the model substantially over-weights its internal confidence relative to the instructed threshold.

Table 11: Qwen 80B: Logistic regression predicting abstention (Phase 4), Full model

Predictor	Coefficient (β)	Std. Error	z	p
Intercept	1.785	0.113	15.83	< .001
Threshold (T)	0.034	0.0009	37.92	< .001
Confidence (%)	-0.051	0.0016	-31.02	< .001
Difficulty	-0.148	0.077	-1.91	.056

Table 12: Qwen 80B: Model comparison for abstention predictions (Phase 4)

Model	AIC (\downarrow)	pseudo- R^2 (\uparrow)	Key Likelihood Ratio Tests
Threshold only (T)	12284.5	0.111	–
Threshold + Confidence	10962.7	0.207	vs. T: $\chi^2(1) = 1323.80$, $p < .001$
Threshold + Difficulty	12062.4	0.127	–
Full (T + Confidence + Difficulty)	10961.1	0.207	vs. T+Conf: $\chi^2(1) = 3.64$, $p = .056$